Intratumoral Treg ablation is sufficient to mediate tumor control systemically without autoimmunity

Alissa Bockman[1], Brenna Gittins[1], Chenyu Zhang[1], Jessica Hung[1], Mariela Moreno Ayala[1], Dorothée Saddier Axe[2], Brian M Weist[2], Michel DuPage[1]
[1]Division of Immunology & Molecular Medicine, Department of Molecular & Cell Biology, University of California, Berkeley;
[2]Gilead Sciences, Inc., 333 Lakeside Drive, Foster City, CA 94404, USA

Contact: dupage@berkeley.edu

ABSTRACT

Regulatory T cells (T_{regs}) infiltrate most tumors, yet whether they suppress immune responses directly within tumor tissues is untested. We used intratumoral (IT) delivery of diphtheria toxin (DT) in *Foxp3*^{DTR} mice to deplete IT T_{regs} while leaving peripheral T_{regs} intact. IT delivery of DT reduced T_{reg} frequencies in the tumor, which promoted potent tumor control without autoimmunity. Interestingly, this control was principally mediated by CD4$^+$ T cells, whereas CD8$^+$ T cells only contributed when CD4$^+$ T cells were absent. While conventional dendritic cells (cDCs) were required to clear tumors, Batf3$^+$ cDC1s were dispensable. Distant secondary tumors, mimicking metastases, were also controlled by IT T_{reg} ablation. Mechanistically, IT T_{regs} suppressed antitumor T cell responses by blocking the acquisition of tumor antigen by cDC2s. Importantly, similar mechanisms of control were observed using a clinically translatable IT T_{reg}-depleting anti-CCR8 antibody and reveal a distinct therapeutic strategy that leverages cDC2s and CD4$^+$ T cells.

INTRODUCTION

High frequencies of tumor-infiltrating regulatory T cells (T_{regs}) are correlated with reduced survival in cancer patients[1–6]. T_{regs} inhibit immune responses through the secretion of suppressive cytokines and the inhibition of costimulatory ligand expression on APCs, among other suppressive mechanisms[7–10]. Eliminating T_{regs} as a therapy is complicated by the fact that T_{regs} are essential for preventing harmful inflammation, including autoimmunity[11–14]. Therefore, to target T_{regs} for the treatment of cancer will require approaches that only disrupt T_{reg} suppression of antitumor immunity while retaining T_{reg} immunoregulatory function in non-tumor tissues.

One approach would be the selective depletion of T_{regs} within tumors, but studies have suggested that T_{regs} may suppress antitumor immune responses outside of the tumor microenvironment[15–19]. Nevertheless, antibody-based strategies that selectively deplete intratumoral (IT) T_{regs} have worked well in mouse models, for example, with antibodies that can deplete intratumoral T_{regs} by targetingCTLA-4, CD25, GITR, 4-1BB, OX-40, LAG3, TIGIT orCCR4[5,10,20–26]. Most recently, T_{regs} were found to upregulate the chemokine receptor CCR8 in tumors from humans and mice[27–31], leading to experiments showing that anti-CCR8 antibodies can effectively control several types

of cancer in mice[32–37]. Currently, phase I and II clinical trials with anti-CCR8 are underway for advanced and metastatic solid cancers (NCT05537740; NCT05101070; NCT06387628; NCT05007782; NCT05635643; NCT05935098). Despite the promise of these new antibody approaches that can selectively deplete IT T_{regs}, the fundamental question as to whether T_{regs} suppressive function occurs only in tumors is not resolved. That is because such antibody approaches cannot be solely restricted to tumor tissues, as cells outside of tumors expressing the target antigen (i.e. CCR8), which include non-T_{reg} cells, may also contribute to tumor control[38–40]. Furthermore, the activation of Fc receptors on immune cells that engage therapeutic antibodies may be critical for the efficacy of these therapeutics[41–43]. Therefore, further research into T_{reg} depletion without using antibodies will directly test whether IT T_{reg} ablation alone directs anti-tumor immunity.

To prevent the activity of antibodies binding to cells outside of the tumor microenvironment, investigators have performed IT delivery of antibodies, as well as immune adjuvants CpG and IL-12-Fc[44–47]. Direct, intratumoral TLR9 activation by CpG injection promoted the control of treated tumors as well as untreated tumors[44]. When TLR9/CpG administration was combined with anti-CTLA4 or anti-OX40 to deplete IT T_{regs}, therapeutic activity was enhanced, leading to effective control of both treated tumors as well as disseminated tumors[44–47]. Intratumoral immunotherapy poses significant clinical benefit, as local delivery may mitigate the autoimmune toxicities that are elicited by systemic drug administrations[48]. However, the role of Fc receptor binding and immune cell activation are still likely to be important, and alternative methods that do not employ antibodies to remove intratumoral T_{regs} must be tested[49].

To directly test whether T_{reg} ablation only within tumors is sufficient to control tumors without inciting autoimmunity, we delivered a low dose of diphtheria toxin directly into tumor tissues by intratumoral diphtheria toxin injection (IT DT) in *FoxP3*^{DTR} mice[11,50]. This technique led to nearly complete ablation of IT T_{regs} while sparing T_{regs} elsewhere throughout the mice. Most importantly, IT T_{reg} ablation by itself led to potent tumor control without inciting autoimmune disease. Furthermore, the ablation of T_{regs} from a single tumor led to control of distant tumors of the same origin that did not receive direct treatments. Unexpectedly, tumor control was dominantly mediated by $CD4^+$ T conventional (Tconv) cells rather than $CD8^+$ T cells, although $CD8^+$ T cells did contribute to tumor control in the absence of $CD4^+$ T cells. In addition, cDC1s were not required for tumor control with IT T_{reg} ablation. Mechanistically, we show that IT T_{regs} suppressed the antitumor response locally by blocking the acquisition of tumor antigen by cDC2s within tumors. We demonstrate enhanced antigen acquisition by cDC2s upon the removal of IT T_{reg} suppression. Similar cell type dependencies were observed with clinically applicable anti-CCR8 intratumoral T_{reg} depleting antibodies. These findings are consequential, as they uncover a clinically relevant mechanism to boost systemic antitumor immune responses that does not rely on $CD8^+$ T cells or cDC1s and is effective without inciting autoimmune toxicity.

RESULTS

Intratumoral T_{reg} depletion controls tumor growth without inciting autoimmunity

It was unclear whether approaches to deplete intratumoral (IT) T_{regs} selectively would have clinical efficacy, as only systemic T_{reg} depletion has been previously tested[51–53]. Several reports have shown that T_{reg} depletion outside of the tumor, e.g. in tumor-draining lymph nodes, is critically important for tumor control[15,16,18,54]. However, recent work has also shown that anti-CCR8 antibodies, which deplete T_{regs} selectively within tumors, prolong mouse survival after challenge with subcutaneously implanted CT26 colorectal carcinoma or EMT6 breast cancer cell lines[32,33]. We confirmed previous findings that T_{regs} within MC38 tumors highly express CCR8 and that anti-CCR8 treatment reduces $CCR8^+$ IT T_{reg} numbers in tumors and significantly decreases MC38 tumor burden (Fig. S1A-G)[27,28,34,36]. Interestingly, anti-CCR8 treatments were not effective against B16F10 tumors (Fig. S1F-G). Overall, these data were consistent with an important role for the local activity of IT T_{regs} in mediating tumor immunotolerance. However, because CCR8 can be expressed on a subset of circulating Tregs and $CD4^+$ T conv cells, it remained possible that anti-CCR8 therapy exerted tumor control by acting more broadly than on IT T_{regs} alone. Furthermore, antibody-mediated cell depletion that activates Fc receptors may have also contributed to the antitumor efficacy[42]. To test whether IT T_{reg} ablation alone is sufficient to promote tumor control without the use of antibodies, we used *FoxP3*^{DTR} mice. However, rather than deliver diphtheria toxin (DT) systemically by intraperitoneal (IP) injection, we delivered low dose DT (250 ng, one-fourth of the dose used IP) directly into tumors (IT) every other day once tumors reached a volume of 50 mm^3 (Fig. 1A). After a single dose of IT DT, IT T_{regs} were efficiently depleted by 48 hours (Fig. 1B). Importantly, we found that IT DT ablation of IT T_{regs} induced significant control of both immune-rich MC38 tumors and poorly immunogenic B16F10 tumors (Fig. 1C,1D).

To determine if IT T_{reg} ablation also promotes tumor control in autochthonous models of cancer, we induced sarcomas in *K-ras*$^{LSL\text{-}G12D}$*;p53*$^{fl/fl}$ ('KP') mice that were bred to the *FoxP3*^{DTR} allele. We dosed *FoxP3*^{DTR}*;K-ras*^{G12D}*;p53*$^{fl/fl}$ with 50,000 infectious units of a lentivirus encoding Cre recombinase (Lenti-x) into the left calf muscle[55,56]. Over the following 150 days, we monitored mice for spontaneous tumor development. When tumors became palpable, mice were administered IT DT as with subcutaneous tumors. We found that IT DT resulted in a significant reduction of IT T_{regs} in this autochthonous tumor setting (Fig. 1E). Ultimately, this reduction in IT T_{regs} was sufficient to extend animal survival, despite the aggressive nature of this tumor model (Fig. 1F). Importantly, Lenti-x-induced sarcomas lack neoantigens recognized by $CD8^+$ T cells and were previously categorized as poorly immunogenic[55,56]. Therefore, IT T_{reg} ablation appeared to promote immune control in a manner independent of a $CD8^+$ T cell response. These results demonstrate a tumor-protective function of IT T_{regs} that is conserved across multiple cancer models.

121 While we observed robust control of IT T_{reg} ablated tumors, we sought to address whether IT T_{reg}
122 ablation also prevented the induction of autoimmune pathologies observed with systemic T_{reg}
123 ablation[11–14,57]. We directly compared *FoxP3*^{DTR} tumor-bearing mice treated with IT DT versus IP
124 DT for a period of 28 days by measuring T_{reg} frequencies, autoimmune pathologies, and the
125 activation status of conventional T cells. First, IP DT treatment induced a significant reduction in
126 T_{reg} frequencies across all tissues analyzed, whereas IT DT impacted T_{reg} frequencies
127 predominantly within the tumor tissue, albeit a moderate T_{reg} reduction was observed in the tumor-
128 draining lymph node (tdLN) (Fig. 2A and Fig. S2A). Second, IP DT treatments significantly
129 increased spleen weight and caused body weight loss in mice with tumors, but IT DT did not (Fig.
130 2B-C; Fig. S2B-C). Furthermore, analysis of hematoxylin and eosin stained sections from the lung,
131 liver, kidney, and heart of IP DT treated mice revealed significant lymphocytic infiltration that
132 was not observed in mice receiving IT DT (Fig. 2D-E, Fig. S2D-E). Third, flow cytometric analysis
133 of CD4$^+$ Tconv and CD8$^+$ T cells from IP DT treated mice, but not IT DT treated mice, revealed
134 robust increases in the expression of CD44, ICOS, CD25, PD1 and TIGIT in the spleen, non-
135 draining lymph nodes (ndLN) and tdLN (Figures 2F-G; Fig. S2F-G). Interestingly, while IT T_{reg}
136 ablation did not induce any sign of systemic autoimmunity, IT T_{reg} ablation did produce more
137 durable and complete rejections (CRs) of tumors compared to systemic T_{reg} ablation by IP DT
138 (Fig. S2H-I). These data demonstrate that IT T_{reg} ablation can control tumors without inducing
139 aberrant immune activation or multi-organ autoimmune disease.
140

141 **Intratumoral T_{reg} depletion promotes CD8+ and CD4+ T cell activation locally in tumors**

142 We next characterized the immunological changes within tumors after IT T_{reg} ablation. While the
143 frequency of CD4$^+$ Tconv cells trended slightly higher with IT T_{reg} ablation, the difference was
144 not statistically significant after 25 days of IT T_{reg} ablation (Fig. 3A). However, we did observe a
145 significant increase in the frequency of CD8$^+$ T cells, as observed by others with anti-CCR8
146 treatment[27,32]. To determine whether IT T_{reg} ablation also increased the frequency of tumor-
147 reactive CD8$^+$ T cells, we stained single cell suspensions collected from IT DT treated tumors with
148 a tetramer specific for the p15E peptide of an endogenous ecotropic murine leukemia virus to
149 detect MC38-specific CD8$^+$ T cells. As has been reported for anti-CCR8 treatments[15,27,33,58–60], we
150 also observed an increased frequency of p15E$^+$CD8$^+$ T cells in tdLNs after IT T_{reg} ablation, but the
151 increase in tumor tissues did not reach significance (Fig. S3A-B). We also noted an increase in
152 effector (CD44+CD62L-) CD4$^+$ and CD8$^+$ T cells in tumor tissue after IT DT (Fig. 3B). We found
153 that IT T_{reg} ablation induced significant upregulation of ICOS and CD25 on IT CD4$^+$ Tconv cells
154 (Fig. 3C and Fig. S3C) and CD8$^+$ T cells (Fig. 3D and Fig. S3D). While the production of TNFα
155 and IFNγ by tumor-infiltrating CD4$^+$ and CD8$^+$ T cells was similar between IT PBS and IT DT
156 treated mice (Fig. 3F and Fig. S3E-I), we observed a significant increase in the frequency of IL-2
157 producing CD4$^+$ Tconv cells after IT T_{reg} ablation (Fig. 3E and Fig. S3J). These results demonstrate
158 that the removal of IT T_{regs} led to an increase in the activation status of conventional CD4$^+$ and
159 CD8$^+$ T cells within tumor tissues. We hypothesize that a reinvigorated T cell pool within tumor
160 tissue is sufficient to promote the tumor control observed with IT T_{reg} ablation.

161
162 **CD4$^+$ T conventional cells can control tumors after IT T$_{reg}$ ablation**
163 It is widely hypothesized that IT T$_{reg}$ ablation unleashes CD8$^+$ T cells to control
164 tumors[15,18,21,27,32,52,58,61]. To directly test the cellular requirements for tumor control after IT T$_{reg}$
165 ablation with IT DT, we performed *in vivo* cellular depletion studies using antibodies against CD4$^+$
166 and CD8$^+$ T cells or natural killer (NK1.1+) cells with IT DT administration (Fig. 4A). Tumor
167 control and survival with IT T$_{reg}$ ablation was unaffected by either CD8$^+$ T cell or NK cell depletion
168 alone (Fig. 4B-E and Fig. S4A-B). However, depletion of CD4$^+$ Tconv cells significantly impaired
169 tumor control and survival with IT T$_{reg}$ ablation. Interestingly, CD8$^+$ T cell depletion in
170 combination with CD4$^+$ T cell depletion fully reversed tumor control with IT T$_{reg}$ ablation. Thus,
171 CD4$^+$ T cells played a primary role in tumor control with IT T$_{reg}$ ablation, while CD8$^+$ T cells only
172 appeared to be required for tumor control in the absence of CD4$^+$ T cells.
173
174 This led us to test whether anti-CCR8 treatment, which is presumed to activate CD8$^+$ T cell
175 responses to tumors[27,32–36], also exhibited similar cellular requirements for tumor control. With
176 anti-CCR8 treatment, tumor control and survival were not prevented by NK or CD8$^+$ T cell
177 depletion alone, but were significantly reversed by depletion of CD4$^+$ T cells, exactly as observed
178 with the IT DT approach (Fig. 4F-G and Fig. S4C). Again, CD8$^+$ T cells only participated in tumor
179 control when CD4$^+$ T cells were also depleted. Thus, despite the robust infiltration and activation
180 of CD8$^+$ T cells with IT T$_{reg}$ ablation, CD8$^+$ T cells do not appear to play a primary role in tumor
181 control on their own. Overall, our findings instead highlight the largely underappreciated role for
182 CD4$^+$ T cells to control tumors without CD8$^+$ T cells, particularly in the context of IT T$_{reg}$ ablation.
183
184 As dendritic cells are integral to initiating and maintaining T cell responses, we next interrogated
185 whether conventional DCs (cDCs) were required for tumor control elicited by IT T$_{reg}$ ablation. We
186 generated *Foxp3^{DTR};Zbtb46^{DTR}* mice and then used their bone marrow to make bone marrow
187 chimeric mice in which T$_{regs}$ and cDCs could be inducibly ablated with DT administration[62,63].
188 Bone marrow chimera mice are required with *Zbtb46^{DTR}* mice due to toxicity observed in intact
189 *Zbtb46^{DTR}* mice[62]. We implanted tumors into these mice and began IT DT treatment once tumors
190 reached ~50 mm^3 (Fig. 4H). Tumor control with IT DT was prevented in mice that lacked cDCs
191 (Fig. 4I). We also found that, in the absence of all cDCs, the increase in frequencies of conventional
192 T cells within tumors that we had observed with IT T$_{reg}$ ablation were prevented (Fig. S4D). These
193 results suggest that cDCs were required for increasing the infiltration or maintenance of T cells
194 within tumor tissues upon IT T$_{reg}$ ablation.
195
196 As cDC1s are well-established as being integral to antitumor immunity in several contexts, such
197 as checkpoint blockade immunotherapies, we next tested whether Batf3$^+$, type I DCs (cDC1s) were
198 required for tumor control with IT T$_{reg}$ ablation[64–67]. We generated *FoxP3^{DTR};Batf3$^{-/-}$* mice and
199 then used IT DT treatment to ablate IT T$_{regs}$ in mice that constitutively lacked cDC1s. We found
200 that cDC1-deficient mice controlled tumors equivalently to control mice (Fig. 4J; Fig. S4E). These

201 data indicate that cDC1s are not important for controlling tumors upon IT T_{reg} ablation and may
202 also support the dispensability for $CD8^+$ T cells previously observed. Further, this finding suggests
203 that cDC2s, which were left intact in *Batf3*$^{-/-}$ mice, may be the critical subtype of cDC required for
204 tumor control with IT T_{reg} ablation.
205
206 **Ablation of IT T_{regs} in a single tumor unleashes antitumor immunity against distal tumors**
207 As disseminated metastatic cancers are in greatest need of treatment and would not be easily
208 treated by IT delivery of agents to all tumors, we wanted to determine whether IT T_{reg} ablation in
209 a single tumor would also boost systemic antitumor immune responses that could control untreated
210 tumors. A precedent exists to support this hypothesis, as local radiation and IT injection of TLR
211 agonists or checkpoint blockade inhibitors have been shown to not only impact the treated tumor,
212 but distal tumors as well[45,47]. To test whether IT T_{reg} ablation alone in a single tumor also imparts
213 control of distal tumors, we inoculated syngeneic tumors on both flanks of *FoxP3*^{DTR} mice. We
214 then initiated IT DT treatment in only one of the two tumors when the average volume of both
215 tumors were ~50 mm^3. In mice with paired MC38 or B16F10 tumors, we found that IT DT
216 treatment of one tumor in each mouse resulted in control of both the treated tumor and the untreated
217 distal tumor (Fig. 5A,B and Fig. S5A-C). Control was only lost in distal tumors when DT treatment
218 ceased due to the rejection of the primary treated tumors. Thus, IT T_{reg} ablation led to systemic
219 control of a distal tumor even though distal tumors were not directly ablated of T_{regs}. These results
220 were indicative of the potential efficacy of IT T_{reg} ablation in a single tumor also controlling distant
221 metastases.
222
223 We hypothesized that the control of the untreated distal tumor resulted from enhanced T cell
224 activation against tumor antigens in the treated tumor that led to a stronger systemic T cell response
225 against the specific tumor, which could target distant untreated tumors due to shared tumor
226 antigens. However, distal tumor control could also be induced if IT T_{reg} ablation led to enhanced
227 inflammation that promoted distinct T cell responses in the distant tumor. To discern which
228 mechanism contributed to distal tumor control, we inoculated individual *FoxP3*^{DTR} mice with two
229 antigenically mismatched tumors, specifically MC38 on one flank and B16F10 on the other, and
230 administered IT DT to only one tumor in each mouse (Fig. 5C). Unlike in mice with matched
231 syngeneic tumors, in these mice with mismatched tumors, IT DT treatment only controlled the
232 treated tumor and not the distal tumor (Fig. 5C). These results indicate that specific immunity
233 generated within the treated tumor, likely reflecting T cell antigen specificity, contributed to the
234 antitumor activity elicited against a distal, syngeneic tumor that was not directly treated.
235 Furthermore, these results confirm that our IT DT approach results in local IT T_{reg} ablation that is
236 restricted to the treated tumors and does not disrupt T_{regs} systemically, consistent with our finding
237 that IT DT treatment does not induce systemic autoimmunity.
238
239 To investigate whether the T cell responses in distal untreated tumors were changed by IT T_{reg}
240 ablation specifically with matched syngeneic tumors, we assessed the frequency and activation

241 state of T cells in the tumors. In matched syngeneic tumors, there was a significant reduction of
242 T_{regs} and an increase in activated ($CD44^+$) $CD8^+$ and $CD4^+$ Tconv cells in the untreated tumors
243 (Fig. 5D). We also observed an upregulation of PD1 and downregulation of CD62L on both T cell
244 subsets in untreated tumors (Fig. S5D-E). However, in mismatched tumors, changes in T_{reg}
245 frequencies and conventional T cell activation status were not observed, supporting the hypothesis
246 that tumor antigen-specific T cell responses were only coordinated in the case of the matched
247 tumors (Fig. 5E, F, Fig. S5F).
248
249 **Control of disseminated tumors is reversed by $CD8^+$ or $CD4^+$ T cell depletions**
250 The impact of IT T_{reg} ablation on infiltration of $CD4^+$ and $CD8^+$ T cells into distant syngeneic
251 tumors suggested that either or both of these populations may participate in distal tumor control.
252 We therefore used cellular depletion studies to establish the immune cell dependencies for distal
253 tumor control (Fig. 6A). As observed with single tumors, depletion of $CD4^+$ T cells reversed the
254 control of the IT T_{reg} ablated tumors as well as the matched distal tumors (Fig. 6B). Interestingly,
255 however, while depleting $CD8^+$ T cells alone did not impede the control of the primary treated
256 tumors (as observed with single tumors, Fig. 4), control of the untreated distal tumor was largely
257 reversed by $CD8^+$ T cell depletion (Fig. 6B). These results demonstrate a context-specific
258 dependency for $CD8^+$ T cells in the control of primary versus disseminated cancer with IT T_{reg}
259 ablation.
260
261 The requirement for $CD8^+$ T cells to control matched disseminated tumors may indicate different
262 cDC requirements for primary versus distal tumor control with IT T_{reg} ablation. Therefore, we
263 again generated *Foxp3*^{DTR};*Zbtb46*^{DTR} bone marrow chimera mice, implanted MC38 tumors on both
264 flanks, and performed IT DT treatment of primary tumors (Fig. 6C). Conditional deletion of both
265 IT T_{regs} and cDCs completely blocked the control of untreated distal tumors as well as the primary
266 tumors (Fig. 6D). These data suggest that enhanced T cell activation observed after IT T_{reg} ablation
267 is dependent upon the presence of cDCs. Given the requirement of $CD8^+$ T cells in controlling
268 tumor progression at a distal site, we expected that cDC1s might contribute to the clearance of dual
269 tumors. However, *FoxP3*^{DTR};*Batf3*$^{-/-}$ mice with dual tumors and IT DT treatment of a primary
270 tumor showed no impairment in the control of either tumor (Fig. 6E, F). Thus, cDCs that do not
271 require Batf3 function were sufficient to promote tumor control with IT T_{reg} ablation, suggesting
272 again that cDC2s may act as the critical mediators of primary and distal tumor control.
273
274 **IT T_{reg} ablation enhances tumor antigen acquisition by cDC2s**
275 To investigate how IT T_{reg} ablation impacted cDCs within the tumor, we implanted MC38 tumor
276 cells that expressed an mCherry fluorescent protein as a trackable tumor antigen[65]. Additionally,
277 we pre-depleted *FoxP3*^{DTR} mice prior to tumor implantation to enhance our ability to detect antigen
278 bearing cDCs. When tumors reached ~50 mm^3, we administered 3 doses of IT DT every other day
279 and at day seven, tumors and tdLNs were analyzed by flow cytometry to quantify immune cells
280 that had phagocytosed fluorescent tumor antigen, in particular cDC1s and cDC2s (Fig. 7A). We

281 found a significant increase in the frequency of mCherry$^+$ CD11c$^+$MHC-II$^+$ DCs in the tumors but
282 not tdLN of IT T_{reg} ablated mice (Fig. 7B and Fig. S6A). Interestingly, by further gating on CD103$^+$
283 cDC1s and CD11b$^+$ cDC2s, we observed that only the cDC2s exhibited significantly increased
284 tumor antigen uptake in tumors upon IT T_{reg} ablation (Fig. 7C and Fig. S6B). In addition, as
285 observed previously with systemic T_{reg} depletion[16,68–70], we observed increased expression of
286 CD80 and CD86 costimulatory ligands on CD11c$^+$MHC-II$^+$ DCs, especially on DCs that were
287 actively phagocytosing tumor antigen (Fig. 7D and Fig. S6C-E). Interestingly, however, we again
288 observed that only the tumor antigen+ cDC2s, and not antigen+ cDC1s, exhibited increased
289 expression of CD80 and CD86 ligands in tumors. This highlights a crucial role for IT T_{regs} in
290 limiting cDC2 tumor antigen uptake and maturation in tumors, which likely leads to reduced
291 antitumor CD4$^+$ and CD8$^+$ antitumor T cell responses.
292
293 To directly test whether cDC2s from tumors exhibited increased phagocytic capacity after IT T_{reg}
294 ablation, we tested tumor single cell suspensions of tumors harvested from IT DT versus IT PBS
295 treated mice for uptake of fluorescent beads *ex vivo* (Fig. 7E). In this assay, we again found that
296 the primary subset of cDCs that had increased phagocytosis of bead antigen in the absence of IT
297 T_{regs} were cDC2s, although IT T_{reg} ablation also enhanced bead uptake in cDC1s, just to a lesser
298 extent (Fig. 7F). These data reveal a novel mechanism by which IT T_{regs} restrict antitumor T cell
299 responses, by restricting tumor antigen uptake locally within tumors. Here, we demonstrate that
300 IT T_{regs} restrict cDC2 uptake of tumor antigen within tumor tissue, thereby dampening CD4$^+$ Tconv
301 cell responses against both local and disseminated tumors. By eliminating T_{regs} within tumors, we
302 found that cDC2 activation and phagocytic capacity were dramatically enhanced, unleashing a
303 CD4$^+$ Tconv cell response that acts independently of cDC1s to control tumors. Thus, intratumoral
304 T_{reg} ablation activates an alternative mechanism of tumor control that depends on cDC2s and CD4$^+$
305 Tconv cells.
306
307 **DISCUSSION**
308 Although modulating T_{reg} function is a key approach to boosting cancer immunotherapy, the role
309 of intratumoral T_{regs} and the mechanisms by which they suppress anti-tumor T cell responses
310 remains incompletely defined. To address this gap in knowledge, we leveraged the *FoxP3^{DTR}*
311 mouse coupled with low-dose IT DT treatment to selectively ablate T_{regs} in tumors. These
312 experiments revealed that T_{reg} suppression within tumor tissue itself is sufficient to promote tumor
313 growth. Importantly, this tumor control occurred without any autoimmune side effects, which are
314 common with T_{reg}-targeting approaches. Removal of IT T_{regs} increased conventional CD4$^+$ and
315 CD8$^+$ T cell activation in tumors. Intriguingly, CD4$^+$ Tconv cells and conventional type II dendritic
316 cells (cDC2s) were primarily responsible for imparting tumor control upon IT T_{reg} ablation. This
317 finding extends to relevant clinical cancer interventions, as we also observed the same critical
318 requirement for CD4$^+$ Tconv cell antitumor responses after anti-CCR8 antibody-mediated IT T_{reg}
319 depletion. These data are consequential, as many combinatorial therapeutics aimed at reducing T_{reg}
320 suppression are thought to act by bolstering antitumor CD8$^+$ T cell responses[15,24,27,52,58,59]. Our data

321 indicate instead that IT T_{reg} suppression primarily restricts $CD4^+$ Tconv cell antitumor immune
322 responses.
323
324 We also establish that local removal of IT T_{reg} suppression unleashes systemic responses against
325 disseminated cancers. These enhanced antitumor responses only occurred when we disrupted IT
326 T_{reg} suppression in a tumor of the same origin as the untreated distal tumor. In the setting of
327 disseminated cancer, however, we found that both $CD8^+$ and CD4+ Tconv cells played an essential
328 role in controlling untreated distal tumors. These findings align with other studies that
329 demonstrated an abscopal therapeutic effect after local IT immunotherapies[45,46,58], but extend such
330 findings by revealing the importance of cDC2s and $CD4^+$ Tconv cells in the control of distal and
331 untreated tumors. Further, our findings are unique in showing that systemic immune responses can
332 be elicited by antibody-independent, non-Fc receptor activating, depletion of IT T_{regs}.
333
334 By disrupting conventional DCs, we also uncovered a critical role for cDCs in promoting T cell
335 responses against tumors. Most cancer immunotherapeutic studies have focused on the role of
336 cDC1s in promoting T cell responses to tumors[71–74]. As such, efforts have focused on targeting the
337 cDC1-CD8 T cell axis in human cancer immunotherapies. Interestingly, we find that IT T_{reg}
338 ablation differs from other modes of T_{reg} targeting, such as by CXCR3-deficiency, which
339 selectively disrupts T_{reg} interactions with cDC1s[65]. While CXCR3+ T_{regs} were shown to selectively
340 impede $CD8^+$ T cell responses against tumors, our data demonstrate that removal of all IT T_{regs} can
341 induce tumor regression through a $CD4^+$ T cell-dependent and cDC1-independent mechanism.
342 Recent literature demonstrates the ability of mature DCs enriched in immunoregulatory molecules
343 (mregDCs) to recruit T_{regs}, allowing for their accumulation around lymphatic vessels in the
344 peripheral tumor stroma[75]. By disrupting this mregDC-T_{reg} axis, tumor immunosurveillance was
345 enhanced[76]. While our data suggest a prominent role for cDC2s in stimulating anti-tumor immune
346 activity, it remains possible that mregDCs may also contribute to tumor rejection in the absence
347 of T_{regs}. Together, these findings are consequential, as they represent a parallel arm of antitumor T
348 cell immune function that may bolster tumor control in cDC1 or $CD8^+$ T cell non-responsive
349 tumors.
350
351 We also show that IT T_{regs} blocked the acquisition of tumor antigens by cDC2s within tumor tissue.
352 In the absence of all cDCs, we abrogated enhanced T cell activation and expansion induced by IT
353 T_{reg} ablation. Others have demonstrated a critical role for cDC2 responses in the tdLN after
354 systemic T_{reg} removal[17]. These studies demonstrated that in the absence of T_{regs}, cDC2s drive
355 strong antitumor responses by picking up tumor antigens, trafficking to tdLNs, and presenting
356 tumor-derived antigens to $CD4^+$ Tconv cells[17,77]. It has also been shown that the abundance of IT
357 cDC2s is correlated with the accumulation of tumor-infiltrating $CD4^+$ Tconv cells in the absence
358 of T_{regs}[66]. While these data established an important role for cDC2s and $CD4^+$ Tconv cells in
359 driving antitumor responses, our data extend these findings to show that enhanced antigen
360 acquisition can occur directly within tumors. Importantly, we also showed that IT T_{reg} ablation, as

361 opposed to systemic T_{reg} ablation, is sufficient to unleash this mechanism of tumor control while
362 also preventing autoimmune pathology.
363
364 Maintenance of immune homeostasis is a vital function of T_{regs}[7,13]. Thus, disrupting global T_{reg}
365 function incurs severe autoimmune disease in humans and in mice[11,12,14]. This motivated our
366 efforts to locally deplete T_{regs} only in tumors to see if this was sufficient for tumor control and
367 would retain critical T_{reg} suppressive functions in peripheral tissues. Although we did not detect
368 changes in $CD4^+$ Tconv or $CD8^+$ T effector function within the tdLN, it remains possible that low-
369 level depletion of tdLN T_{regs} contributes to antitumor immunity. However, our data that show loss
370 of tumor control when distant tumors are mismatched from a treated tumor suggests that IT T_{reg}
371 ablation was acting locally within tumors. Thus, our results support the feasibility of strategies that
372 selectively disrupt IT T_{regs} for safe and effective cancer immunotherapy.
373
374 Current clinical data demonstrate poor prognostic outcomes in tumors that are cDC1 or $CD8^+$ T
375 cell low[78,79]. These tumors have been shown to respond poorly to anti-PD-1 checkpoint blockade
376 as well as other immunotherapies[74,80,81]. In these cases, failed tumor immunosurveillance was
377 attributed to the downregulation of MHC I molecules on the tumor cell surface, or the absence of
378 tumor neoantigens, capable of eliciting CD8 T cell responses[82–85]. Our data identify a novel
379 mechanism to combat CD8-resistant tumors, or synergize with such existing therapeutic strategies,
380 by unleashing cDC2s and $CD4^+$ T cell-mediated tumor control by IT T_{reg} ablation.
381
382 Here, we show that IT T_{reg} ablation is sufficient to promote tumor control and we uncover a novel
383 function of IT T_{reg} function that suppresses cDC tumor antigen uptake. IT T_{reg} function suppresses
384 effective $CD4^+$ Tconv cell responses locally in tumors and disrupts the ability of both $CD4^+$ and
385 $CD8^+$ T cells to cooperate in the control of distant untreated tumors. Our findings also extend to a
386 clinically viable mode of IT T_{reg} depletion using an anti-CCR8 antibody delivered systemically.
387 These data are consequential, as they demonstrate a novel arm of adaptive immunity that can be
388 leveraged to enhance the immunotherapeutic treatment of patients with cancer.
389
390

391 # Methods
392 All of the experiments were conducted according to the Institutional Animal Care and Use
393 Committee guidelines of the University of California, Berkeley. Further information on the
394 committees that approved protocols used in this publication can be found in each corresponding
395 section.
396
397 ***In vivo* animal studies**
398 Mice used were bred onto a C57BL/6 background for a minimum of ten generations. Littermates
399 or age-matched control mice (8-20 weeks old) were used in all mouse experiments. *Foxp3*$^{GFP\text{-}DTR}$
400 mice express human diphtheria toxin receptor and EGFP genes from the Foxp3 locus without
401 disrupting expression of the endogenous FoxP3 gene[11]. These mice were a gift from Dr. Rudensky
402 (Memorial Sloan Kettering Institute; JAX:016958). *Foxp3*$^{GFP\text{-}DTR}$*;Kras*^{G12D}*;p53*$^{fl/fl}$ mice were
403 kindly provided by Dr. Jacks (Massachusetts Institute of Technology). *Zbtb46*^{DTR} mice were
404 originally characterized by Dr. Nussenzweig (Rockefeller University) and *Batf3*$^{-/-}$ mice were
405 characterized by Dr. Murphy (Washington University School of Medicine). Both *Zbtb46*^{DTR} mice
406 and *Batf3*$^{-/-}$ mice were obtained from Jackson laboratories (JAX:019506; and JAX:013755,
407 respectively) and backcrossed with *Foxp3*$^{GFP\text{-}DTR}$ mice in our laboratory. For diphtheria toxin
408 treatments, mice were injected with 1 μg intraperitoneal (IP) or 250 ng intratumoral (IT) every
409 other day up to three times per week. For syngeneic tumor studies, C57BL/6 mice were
410 subcutaneously inoculated in 100uL of PBS with $5x10^5$ MC38 cells or $5x10^5$ B16F10 cells. For
411 autochthonous tumor studies, sarcomas were induced in *Foxp3*$^{GFP\text{-}DTR}$*;Kras*^{G12D}*;p53*$^{fl/fl}$ mice by
412 intramuscular (IM) injection of the hind calf muscle with replication-incompetent lentiviruses
413 express Cre recombinase as reported prevoiusly[56,86]. Mice were monitored three times per week
414 for palpable sarcoma formation beginning 50 days after IM injection. Tumor measurements were
415 performed blindly using calipers three times per week. A single operator measured each tumor in
416 three dimensions for each tumor measurement. All experiments were performed in accordance
417 with the Institutional Laboratory Animal Care and Use Committee (IACUC) and the Office of
418 Laboratory Animal Care (OLAC) at the University of California, Berkeley.
419
420 **Lentiviral production**
421 293T cells were transfected with d8.2 (gag/pol), CMV-VSV-G and a transfer vector expressing
422 Cre to produce lentivirus.
423
424 **Cell lines**
425 MC38 and B16F10 cell lines were kindly provided by Dr. Bluestone (UCSF). All MC38 cell lines
426 expressed luciferase with or without co-expression of mCherry. All cell lines were maintained in
427 DMEM (GIBCO) supplemented with 10% FBS, sodium pyruvate (GIBCO), 10mM HEPES
428 (GIBCO), and penicillin-streptomycin (GIBCO). Tumor cells were grown at 37C with 5% CO_2.
429
430 **Murine Lymphocyte isolation**

431 Single cell suspensions were generated from lymphoid organs through mechanical disruption of
432 harvested tissues and were passed through 40um filters. Suspensions were resuspended in ice-cold
433 FACS buffer (PBS supplemented with 2mM EDTA and 2% FBS). Spleens were subjected to red
434 blood cell lysis using ACK lysis buffer (150mM NH4Cl, 10mM KHCO3, 0.1mM NA2EDTA, pH
435 7.3). Resected tumors were minced to 1mm3 isolates and digested in RPMI media supplemented
436 with 4-(2-hydroxyethyl)-1-piperazineethanesulfonic acid (HEPES), 20mg/mL DNase I (Roche),
437 and 125U/mL collagenase D (Roche). Tumor isolates were digested in an orbital shaker for 45
438 minutes at 37C. All cell suspensions were passed through 40um filters before cell staining or in
439 vitro stimulation. Cytokine staining was performed on 3-5x10^6 cells, after 210 minutes of *in vitro*
440 stimulation in Opti-MEM media supplemented with Brefeldin A (eBioscience), 10ng/mL phorbol
441 12-myristate 13-acetate (PMA)(Sigma), and 0.25uM ionomycin (Sigma). Fixation and
442 permeabilization of cells was performed for intracellular staining using the Tonbo Foxp3
443 Transcription Factor Staining Buffer Kit. In some experiments, e.g. staining of APCs for in vivo
444 acquisition of mCherry tumor antigen, cells were fixed with 4% PFA on ice for 15 minutes.
445
446 **Flow cytometry**
447 Flow cytometry was performed on a BD LSR Fortessa X20 (BD Biosciences) and datasets were
448 analyzed using FlowJo software (Tree Star). All samples analyzed were reconstituted in single cell
449 suspensions using ice-cold FACS buffer (PBS with 2mM EDTA and 2% FBS). Dead cells were
450 stained with Live/Dead Fixable Blue or Aqua Dead Cell Stain kit (Molecular Probes) in PBS for
451 20 minutes at 4C. Cell surface proteins were stained for 20 minutes at 4C using a mixture of
452 fluorophore-conjugated antibodies. Surface marker stains for murine samples were carried out
453 with anti-mouse CD4 (RM4-5, BioLegend), anti-mouse CD8a (53-6.7, BioLegend), anti-CD25
454 (PC61, BioLegend), anti-mouse CD44 (IM7, BioLeged), anti-mouse CD45 (30-F11, BioLegend),
455 anti-mouse CD103 (2E7, BioLegend), anti-mouse PD1 (29F.1A12, BioLegend), anti-mouse
456 CCR8 (SA214G2, Biolegend), anti-mouse MHCII (M5/114.15.2, BioLegend), anti-H-2Kb MuLV
457 p15E Tetramer-KSPWFTTL (NIH tetramer core), anti-mouse TIGIT (Vstm3, Biolegend), anti-
458 mouse ICOS (C398.4A, Biolegend), anti-mouse CD62L (MEL1-14, Biolegend) anti-mouse
459 CD11b (M1/70, Biolegend), anti-mouse CD3e (17A2, Biolegend), anti-mouse B220 (FA3-6B2,
460 Biolegend), anti-mouse F4/80 (BM8, Biolegend), anti-mouse CD80 (M16-10A1, Biolegend), anti-
461 mouse CD86 (GL-1, Biolegend) and anti-mouse PD-L1 (10F.9G2, Biolegend). anti-mouse CD11c
462 (N418, Biolegend) in PBS for 20 minutes at 4C. Cells were fixed using the Tonbo Foxp3
463 Transcription Factor Staining Buffer Kit, prior to intracellular staining. Intracellular staining was
464 performed using anti-mouse anti-mouse Foxp3 (FJK-16S, eBioscience), anti-mouse IL-2 (JES6-
465 5H4, Biolegend), anti-mouse TNF-a (MP6-XT22, BioLegend), anti-mouse IL-10 (JES5-16E3,
466 Biolegend), anti-mouse IFNg (XMG1.2, eBioscience) in PBS for 1 hour at 4C, according to
467 manufacturer's instructions. Cells were resuspended in FACS buffer and filtered through a 40-mm
468 nylon mesh before data acquisition.
469
470 **In vivo antibody-mediated cell depletion**

Immune cell depletion of CD8+ T cells, CD4+ T cells or NK cells was achieved through intraperitoneal injection of 200ug per mouse of each respective depleting antibody. Antibody-based depletion was started at the time of IT DT and was readministered every 6 days throughout the study. CD8b.2 (Clone 53-5.8, Leinco Technologies, Catalog # C2832) was used for CD8+ T cell depletions. Clone GK1.4 (Leinco Technologies, Catalog #C1333) was used for CD4+ T cell depletions. Clone PK136 (Leinco Technologies, Catalog #N123) was used for NK cell depletions. Anti-CCR8 mIgG2a (Gilead Sciences) was administered at 200 ug IP seven days after tumor inoculation and was re-dosed every 3 days.

Bone marrow chimera generation

Host CD45.1+ C57/BL6 mice were administered two doses of 5 Gy irradiation, 16 hours apart. An Xrad320 (Precision X-Ray Irradiation) was used to administer irradiation. 4 hours after the second irradiation treatment, 10x106 bone marrow cells were transferred to host mice via tail vein injection. Bone marrow was harvested from donor *Zbtb46*^{DTR}, *Foxp3*^{DTR}, or *Zbtb46*^{DTR}*Foxp3*^{DTR} CD45.2+ C57/BL6 mice. Femurs and tibias were harvested from euthanized donor mice and flushed with ice-cold RPMI supplemented with 2% FBS, using a 27-gauge syringe. Red blood cells were removed from bone marrow preparations by using ACK lysis buffer (150mM NH4Cl, 10mM KHCO3, 0.1mM NA2EDTA, pH 7.3). Bone marrow was then washed with ice-cold PBS three times prior to tail vein injection. After bone marrow transfer, mice were administered water supplemented with sulfamethoxazole-trimethoprim oral suspension (Ani Pharmaceuticals) for 30 days and were monitored daily. Bone marrow was permitted to reconstitute recipient mice for 60 days. Following reconstitution, $5x10^5$ MC38 tumor cells were subcutaneously inoculated. 7 days after tumor inoculation, mice were administered either IT PBS or a combination of 250 ng IT DT and 80 ng intraperitoneal DT.

Statistical methods

p values were obtained from unpaired two-tailed Student's t tests for all statistical comparisons between two groups, and data were displayed as mean ± SEMs. For multiple comparisons, one-way ANOVA was used. For tumor growth curves, two-way ANOVA was used with Tukey's multiple comparisons test performed at each time point or by multiple regression analysis. Survival analysis was performed using one-way chi-square test or Log-rank (Mantel-Cox) test. p values are denoted in figures by $*p < 0.05$, $**p < 0.01$, and $***p < 0.001$.

Data availability

Values Data supporting the findings of this study are available within the article and supplementary files or from the corresponding authors upon request. Source data are provided with this paper.

507 ## References

508 1. Curiel, T. J. *et al.* Specific recruitment of regulatory T cells in ovarian carcinoma fosters
509 immune privilege and predicts reduced survival. *Nat. Med.* **10**, 942–949 (2004).
510 2. Fridman, W. H., Pagès, F., Sautès-Fridman, C. & Galon, J. The immune contexture in
511 human tumours: impact on clinical outcome. *Nat. Rev. Cancer* **12**, 298–306 (2012).
512 3. Jensen, H. K., Donskov, F., Nordsmark, M., Marcussen, N. & von der Maase, H. Increased
513 intratumoral FOXP3-positive regulatory immune cells during interleukin-2 treatment in
514 metastatic renal cell carcinoma. *Clin. Cancer Res.* **15**, 1052–1058 (2009).
515 4. Sasaki, A. *et al.* Prognostic value of tumor-infiltrating FOXP3+ regulatory T cells in
516 patients with hepatocellular carcinoma. *Eur. J. Surg. Oncol.* **34**, 173–179 (2008).
517 5. Tao, H. *et al.* Prognostic potential of FOXP3 expression in non-small cell lung cancer cells
518 combined with tumor-infiltrating regulatory T cells. *Lung Cancer* **75**, 95–101 (2012).
519 6. Shang, B., Liu, Y., Jiang, S.-J. & Liu, Y. Prognostic value of tumor-infiltrating FoxP3+
520 regulatory T cells in cancers: a systematic review and meta-analysis. *Sci. Rep.* **5**, 15179
521 (2015).
522 7. Dikiy, S. & Rudensky, A. Y. Principles of regulatory T cell function. *Immunity* **56**, 240–255
523 (2023).
524 8. Togashi, Y., Shitara, K. & Nishikawa, H. Regulatory T cells in cancer immunosuppression -
525 implications for anticancer therapy. *Nat. Rev. Clin. Oncol.* **16**, 356–371 (2019).
526 9. Tay, C., Tanaka, A. & Sakaguchi, S. Tumor-infiltrating regulatory T cells as targets of
527 cancer immunotherapy. *Cancer Cell* **41**, 450–465 (2023).
528 10. Shan, F., Somasundaram, A., Bruno, T. C., Workman, C. J. & Vignali, D. A. A. Therapeutic
529 targeting of regulatory T cells in cancer. *Trends Cancer* **8**, 944–961 (2022).

530 11. Kim, J. M., Rasmussen, J. P. & Rudensky, A. Y. Regulatory T cells prevent catastrophic
531 autoimmunity throughout the lifespan of mice. *Nat. Immunol.* **8**, 191–197 (2007).
532 12. Bennett, C. L. *et al.* The immune dysregulation, polyendocrinopathy, enteropathy, X-linked
533 syndrome (IPEX) is caused by mutations of FOXP3. *Nat. Genet.* **27**, 20–21 (2001).
534 13. Sakaguchi, S., Yamaguchi, T., Nomura, T. & Ono, M. Regulatory T cells and immune
535 tolerance. *Cell* **133**, 775–787 (2008).
536 14. Sakaguchi, S., Sakaguchi, N., Asano, M., Itoh, M. & Toda, M. Immunologic self-tolerance
537 maintained by activated T cells expressing IL-2 receptor alpha-chains (CD25). Breakdown
538 of a single mechanism of self-tolerance causes various autoimmune diseases. *J. Immunol.*
539 **155**, 1151–1164 (1995).
540 15. Zhou, X. *et al.* Precise spatiotemporal interruption of regulatory T-cell-mediated CD8+ T-
541 cell suppression leads to tumor immunity. *Cancer Res.* **79**, 585–597 (2019).
542 16. Zagorulya, M. *et al.* Tissue-specific abundance of interferon-gamma drives regulatory T
543 cells to restrain DC1-mediated priming of cytotoxic T cells against lung cancer. *Immunity*
544 **56**, 386–405.e10 (2023).
545 17. Binnewies, M. *et al.* Unleashing type-2 dendritic cells to drive protective antitumor CD4+ T
546 cell immunity. *Cell* **177**, 556–571.e16 (2019).
547 18. Deng, L. *et al.* Accumulation of foxp3+ T regulatory cells in draining lymph nodes
548 correlates with disease progression and immune suppression in colorectal cancer patients.
549 *Clin. Cancer Res.* **16**, 4105–4112 (2010).
550 19. Núñez, N. G. *et al.* Tumor invasion in draining lymph nodes is associated with Treg
551 accumulation in breast cancer patients. *Nat. Commun.* **11**, 3272 (2020).
552 20. Tanaka, A. & Sakaguchi, S. Targeting Treg cells in cancer immunotherapy. *Eur. J.*

553 *Immunol.* **49**, 1140–1146 (2019).

554 21. Selby, M. J. *et al.* Anti-CTLA-4 antibodies of IgG2a isotype enhance antitumor activity
555 through reduction of intratumoral regulatory T cells. *Cancer Immunol. Res.* **1**, 32–42
556 (2013).

557 22. Simpson, T. R. *et al.* Fc-dependent depletion of tumor-infiltrating regulatory T cells co-
558 defines the efficacy of anti-CTLA-4 therapy against melanoma. *J. Exp. Med.* **210**, 1695–
559 1710 (2013).

560 23. Liu, C., Workman, C. J. & Vignali, D. A. A. Targeting regulatory T cells in tumors. *FEBS*
561 *J.* **283**, 2731–2748 (2016).

562 24. Piconese, S., Valzasina, B. & Colombo, M. P. OX40 triggering blocks suppression by
563 regulatory T cells and facilitates tumor rejection. *J. Exp. Med.* **205**, 825–839 (2008).

564 25. Sugiyama, D. *et al.* Anti-CCR4 mAb selectively depletes effector-type FoxP3+CD4+
565 regulatory T cells, evoking antitumor immune responses in humans. *Proc. Natl. Acad. Sci.*
566 *U. S. A.* **110**, 17945–17950 (2013).

567 26. Marshall, L. A. *et al.* Tumors establish resistance to immunotherapy by regulating Treg
568 recruitment via CCR4. *J. Immunother. Cancer* **8**, e000764 (2020).

569 27. Haruna, M. *et al.* The impact of CCR8+ regulatory T cells on cytotoxic T cell function in
570 human lung cancer. *Sci. Rep.* **12**, 5377 (2022).

571 28. Whiteside, S. K. *et al.* CCR8 marks highly suppressive Treg cells within tumours but is
572 dispensable for their accumulation and suppressive function. *Immunology* **163**, 512–520
573 (2021).

574 29. Soler, D. *et al.* CCR8 expression identifies CD4 memory T cells enriched for FOXP3+
575 regulatory and Th2 effector lymphocytes. *J. Immunol.* **177**, 6940–6951 (2006).

576 30. De Simone, M. *et al.* Transcriptional landscape of human tissue lymphocytes unveils
577 uniqueness of tumor-infiltrating T regulatory cells. *Immunity* **45**, 1135–1147 (2016).
578 31. Plitas, G. *et al.* Regulatory T cells exhibit distinct features in human breast cancer. *Immunity*
579 **45**, 1122–1134 (2016).
580 32. Villarreal, D. O. *et al.* Targeting CCR8 induces protective antitumor immunity and
581 enhances vaccine-induced responses in colon cancer. *Cancer Res.* **78**, 5340–5348 (2018).
582 33. Van Damme, H. *et al.* Therapeutic depletion of CCR8+ tumor-infiltrating regulatory T cells
583 elicits antitumor immunity and synergizes with anti-PD-1 therapy. *J. Immunother. Cancer*
584 **9**, e001749 (2021).
585 34. Campbell, J. R. *et al.* Fc-optimized anti-CCR8 antibody depletes regulatory T cells in
586 human tumor models. *Cancer Res.* **81**, 2983–2994 (2021).
587 35. Wang, T. *et al.* CCR8 blockade primes anti-tumor immunity through intratumoral
588 regulatory T cells destabilization in muscle-invasive bladder cancer. *Cancer Immunol.*
589 *Immunother.* **69**, 1855–1867 (2020).
590 36. Weaver, J. D. *et al.* Differential expression of CCR8 in tumors versus normal tissue allows
591 specific depletion of tumor-infiltrating T regulatory cells by GS-1811, a novel Fc-optimized
592 anti-CCR8 antibody. *Oncoimmunology* **11**, 2141007 (2022).
593 37. Kidani, Y. *et al.* CCR8-targeted specific depletion of clonally expanded Treg cells in tumor
594 tissues evokes potent tumor immunity with long-lasting memory. *Proc. Natl. Acad. Sci. U.*
595 *S. A.* **119**, e2114282119 (2022).
596 38. Jacobs, J. F. M. *et al.* Dendritic cell vaccination in combination with anti-CD25 monoclonal
597 antibody treatment: a phase I/II study in metastatic melanoma patients. *Clin. Cancer Res.*
598 **16**, 5067–5078 (2010).

599 39. Doi, T. *et al.* A phase I study of the anti-CC chemokine receptor 4 antibody,
600 mogamulizumab, in combination with nivolumab in patients with advanced or metastatic
601 solid tumors. *Clin. Cancer Res.* **25**, 6614–6622 (2019).
602 40. Sharma, A. *et al.* Anti-CTLA-4 immunotherapy does not deplete FOXP3+ regulatory T
603 cells (tregs) in human cancers. *Clin. Cancer Res.* **25**, 1233–1238 (2019).
604 41. Bulliard, Y. *et al.* Activating Fc γ receptors contribute to the antitumor activities of
605 immunoregulatory receptor-targeting antibodies. *J. Exp. Med.* **210**, 1685–1693 (2013).
606 42. Yofe, I. *et al.* Anti-CTLA-4 antibodies drive myeloid activation and reprogram the tumor
607 microenvironment through FcγR engagement and type I interferon signaling. *Nat. Cancer* **3**,
608 1336–1350 (2022).
609 43. Dahan, R. *et al.* Therapeutic activity of agonistic, human anti-CD40 monoclonal antibodies
610 requires selective FcγR engagement. *Cancer Cell* **29**, 820–831 (2016).
611 44. Miller, C. L. *et al.* Targeted TLR9 agonist elicits effective antitumor immunity against
612 spontaneously arising breast tumors. *J. Immunol.* **211**, 295–305 (2023).
613 45. Hong, W. X., Sagiv-Barfi, I., Czerwinski, D. K., Sallets, A. & Levy, R. Neoadjuvant
614 intratumoral immunotherapy with TLR9 activation and anti-OX40 antibody eradicates
615 metastatic cancer. *Cancer Res.* **82**, 1396–1408 (2022).
616 46. Marabelle, A. *et al.* Depleting tumor-specific Tregs at a single site eradicates disseminated
617 tumors. *J. Clin. Invest.* **123**, 2447–2463 (2013).
618 47. Sagiv-Barfi, I., Czerwinski, D. K., Shree, T., Lohmeyer, J. J. K. & Levy, R. Intratumoral
619 immunotherapy relies on B and T cell collaboration. *Sci. Immunol.* **7**, eabn5859 (2022).
620 48. Hong, W. X. *et al.* Intratumoral immunotherapy for early-stage solid tumors. *Clin. Cancer*
621 *Res.* **26**, 3091–3099 (2020).

622 49. Guan, X. *et al.* Anti-TIGIT antibody improves PD-L1 blockade through myeloid and Treg
623 cells. *Nature* **627**, 646–655 (2024).
624 50. Bos, P. D., Plitas, G., Rudra, D., Lee, S. Y. & Rudensky, A. Y. Transient regulatory T cell
625 ablation deters oncogene-driven breast cancer and enhances radiotherapy. *J. Exp. Med.* **210**,
626 2435–2466 (2013).
627 51. Pastille, E. *et al.* Transient ablation of regulatory T cells improves antitumor immunity in
628 colitis-associated colon cancer. *Cancer Res.* **74**, 4258–4269 (2014).
629 52. Teng, M. W. L. *et al.* Multiple antitumor mechanisms downstream of prophylactic
630 regulatory T-cell depletion. *Cancer Res.* **70**, 2665–2674 (2010).
631 53. Shimizu, J., Yamazaki, S. & Sakaguchi, S. Induction of tumor immunity by removing
632 CD25+CD4+ T cells: a common basis between tumor immunity and autoimmunity. *J.*
633 *Immunol.* **163**, 5211–5218 (1999).
634 54. Piersiala, K. *et al.* Tumour-draining lymph nodes in head and neck cancer are characterized
635 by accumulation of CTLA-4 and PD-1 expressing Treg cells. *Transl. Oncol.* **23**, 101469
636 (2022).
637 55. DuPage, M., Mazumdar, C., Schmidt, L. M., Cheung, A. F. & Jacks, T. Expression of
638 tumour-specific antigens underlies cancer immunoediting. *Nature* **482**, 405–409 (2012).
639 56. DuPage, M. *et al.* Endogenous T cell responses to antigens expressed in lung
640 adenocarcinomas delay malignant tumor progression. *Cancer Cell* **19**, 72–85 (2011).
641 57. Joshi, N. S. *et al.* Regulatory T cells in tumor-associated tertiary lymphoid structures
642 suppress anti-tumor T cell responses. *Immunity* **43**, 579–590 (2015).
643 58. Fransen, M. F., van der Sluis, T. C., Ossendorp, F., Arens, R. & Melief, C. J. M. Controlled
644 local delivery of CTLA-4 blocking antibody induces CD8+ T-cell-dependent tumor

645 eradication and decreases risk of toxic side effects. *Clin. Cancer Res.* **19**, 5381–5389
646 (2013).
647 59. Geels, S. N. *et al.* Interruption of the intratumor CD8+ T cell:Treg crosstalk improves the
648 efficacy of PD-1 immunotherapy. *Cancer Cell* **42**, 1051–1066.e7 (2024).
649 60. Takahashi, M. *et al.* Intratumoral antigen signaling traps CD8+ T cells to confine
650 exhaustion to the tumor site. *Sci. Immunol.* **9**, eade2094 (2024).
651 61. Zhou, L. *et al.* Spatial and functional targeting of intratumoral Tregs reverses CD8+ T cell
652 exhaustion and promotes cancer immunotherapy. *J. Clin. Invest.* **134**, (2024).
653 62. Meredith, M. M. *et al.* Expression of the zinc finger transcription factor zDC (Zbtb46,
654 Btbd4) defines the classical dendritic cell lineage. *J. Exp. Med.* **209**, 1153–1165 (2012).
655 63. Satpathy, A. T. *et al.* Zbtb46 expression distinguishes classical dendritic cells and their
656 committed progenitors from other immune lineages. *J. Exp. Med.* **209**, 1135–1152 (2012).
657 64. Zagorulya, M. & Spranger, S. Once upon a prime: DCs shape cancer immunity. *Trends*
658 *Cancer* **9**, 172–184 (2023).
659 65. Moreno Ayala, M. A. *et al.* CXCR3 expression in regulatory T cells drives interactions with
660 type I dendritic cells in tumors to restrict CD8+ T cell antitumor immunity. *Immunity* **56**,
661 1613–1630.e5 (2023).
662 66. Pittet, M. J., Di Pilato, M., Garris, C. & Mempel, T. R. Dendritic cells as shepherds of T cell
663 immunity in cancer. *Immunity* **56**, 2218–2230 (2023).
664 67. Yin, X., Chen, S. & Eisenbarth, S. C. Dendritic cell regulation of T helper cells. *Annu. Rev.*
665 *Immunol.* **39**, 759–790 (2021).
666 68. Qureshi, O. S. *et al.* Trans-endocytosis of CD80 and CD86: a molecular basis for the cell-
667 extrinsic function of CTLA-4. *Science* **332**, 600–603 (2011).

668 69. Wing, K. *et al.* CTLA-4 control over Foxp3+ regulatory T cell function. *Science* **322**, 271–
669 275 (2008).
670 70. He, X. & Xu, C. Immune checkpoint signaling and cancer immunotherapy. *Cell Res.* **30**,
671 660–669 (2020).
672 71. Spranger, S., Dai, D., Horton, B. & Gajewski, T. F. Tumor-residing Batf3 dendritic cells are
673 required for effector T cell trafficking and adoptive T cell therapy. *Cancer Cell* **31**, 711–
674 723.e4 (2017).
675 72. Broz, M. L. *et al.* Dissecting the tumor myeloid compartment reveals rare activating
676 antigen-presenting cells critical for T cell immunity. *Cancer Cell* **26**, 938 (2014).
677 73. Hildner, K. *et al.* Batf3 deficiency reveals a critical role for CD8alpha+ dendritic cells in
678 cytotoxic T cell immunity. *Science* **322**, 1097–1100 (2008).
679 74. Salmon, H. *et al.* Expansion and activation of CD103(+) dendritic cell progenitors at the
680 tumor site enhances tumor responses to therapeutic PD-L1 and BRAF inhibition. *Immunity*
681 **44**, 924–938 (2016).
682 75. Maier, B. *et al.* A conserved dendritic-cell regulatory program limits antitumour immunity.
683 *Nature* **580**, 257–262 (2020).
684 76. You, S. *et al.* Lymphatic-localized Treg-mregDC crosstalk limits antigen trafficking and
685 restrains anti-tumor immunity. *Cancer Cell* **42**, 1415–1433.e12 (2024).
686 77. Xiao, L. *et al.* Adoptively transferred tumor-specific IL-9-producing cytotoxic CD8+ T cells
687 activate host CD4+ T cells to control tumors with antigen loss. *Nat. Cancer* **6**, 718–735
688 (2025).
689 78. Ho, W. W. *et al.* Dendritic cell paucity in mismatch repair-proficient colorectal cancer liver
690 metastases limits immune checkpoint blockade efficacy. *Proc. Natl. Acad. Sci. U. S. A.* **118**,

691 e2105323118 (2021).
692 79. Budhu, A. *et al.* Tumor biology and immune infiltration define primary liver cancer subsets
693 linked to overall survival after immunotherapy. *Cell Rep. Med.* **4**, 101052 (2023).
694 80. Hegde, S. *et al.* Dendritic cell paucity leads to dysfunctional immune surveillance in
695 pancreatic cancer. *Cancer Cell* **37**, 289–307.e9 (2020).
696 81. Hashimoto, M., Ramalingam, S. S. & Ahmed, R. Harnessing CD8 T cell responses using
697 PD-1-IL-2 combination therapy. *Trends Cancer* **10**, 332–346 (2024).
698 82. Taylor, B. C. & Balko, J. M. Mechanisms of MHC-I downregulation and role in
699 immunotherapy response. *Front. Immunol.* **13**, 844866 (2022).
700 83. Schumacher, T. N. & Schreiber, R. D. Neoantigens in cancer immunotherapy. *Science* **348**,
701 69–74 (2015).
702 84. MacNabb, B. W. *et al.* Dendritic cells can prime anti-tumor CD8+ T cell responses through
703 major histocompatibility complex cross-dressing. *Immunity* **55**, 2206–2208 (2022).
704 85. McGranahan, N. *et al.* Allele-specific HLA loss and immune escape in lung cancer
705 evolution. *Cell* **171**, 1259–1271.e11 (2017).
706 86. Kirsch, D. G. *et al.* A spatially and temporally restricted mouse model of soft tissue
707 sarcoma. *Nat. Med.* **13**, 992–997 (2007).

708 **Acknowledgements**

709 We thank David Raulet, Ellen Robey, Greg Barton and members of the DuPage laboratory for
710 reviewing the manuscript and providing feedback. We also thank Hector Nolla, Alma Valleros,
711 Kartoosh Heydari, Melaine Delcroix and Harman Dhaliwal of the UC Berkeley Cancer Research
712 Laboratory Flow Cytometry Facility. Furthermore, we thank all the members of the DuPage lab
713 for providing guidance on the research approach. M.D is a Pew-Stewart Scholar and a St.
714 Baldrick's Scholar with generous support from Hope with Hazel.
715

716 **Author Contributions**

Conceptualization and methodology, M.D. and A.B.; Investigation, A.B., B.G. and M.D.; writing - original draft, M.D. and A.B; writing - review & editing, M.D., A.B., B.G., C.Z.; supervision, M.D. and A.B.; funding acquisition, M.D.

Competing Interests

M.D. is supported by Gilead Sciences, which provided funding and anti-CCR8 antibody reagents that supported this work. The other authors declare no competing interests.

Additional information

Correspondence and requests for materials should be addressed to Alissa Bockman or Michel DuPage.

FIGURE 1

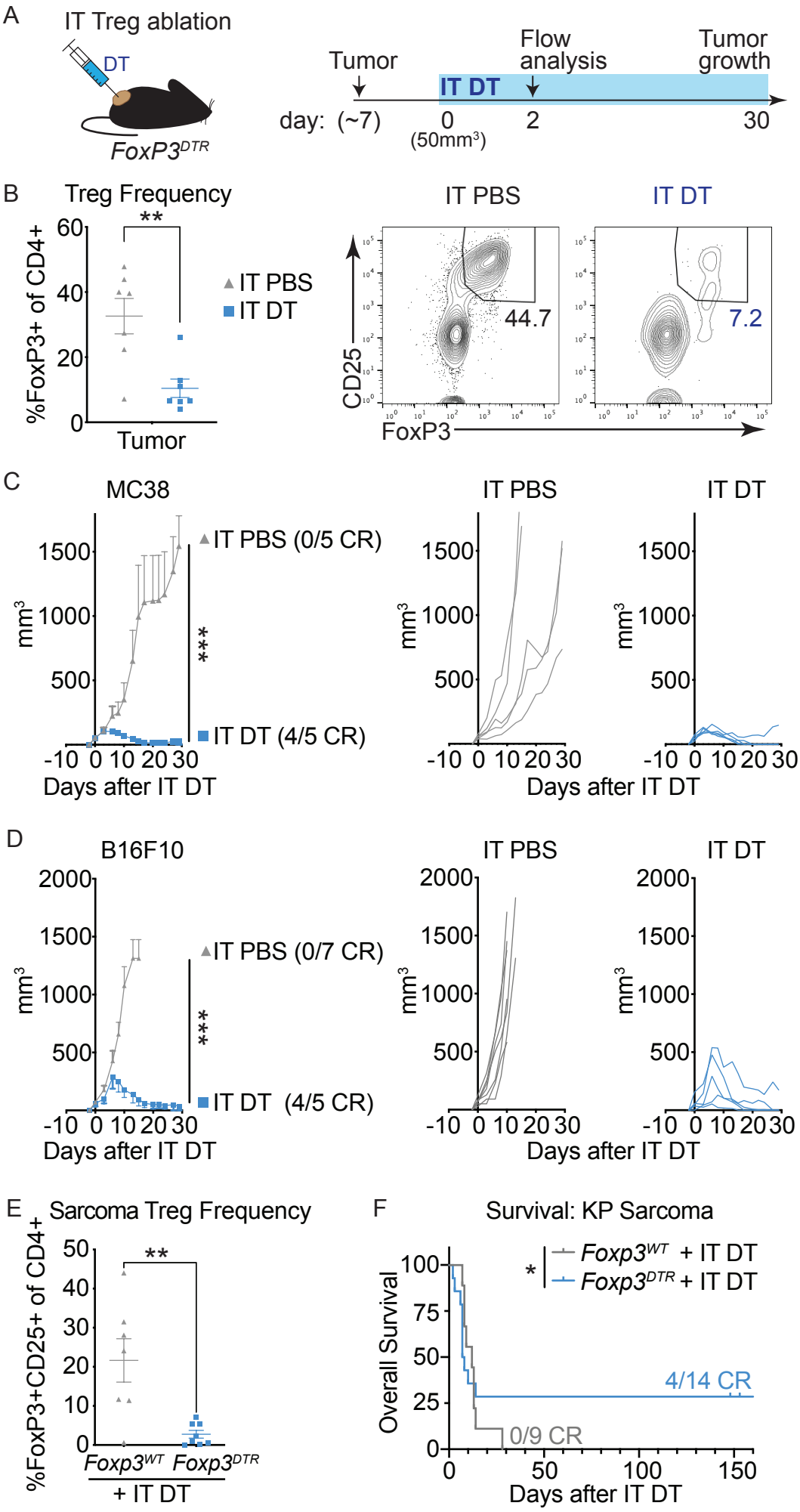
A
IT Treg ablation
DT
FoxP3DTR
Tumor
Flow analysis
Tumor growth
IT DT
day: (~7)
0
(50mm3)
2
30
B
Treg Frequency
%FoxP3+ of CD4+
60
40
20
0
**
Tumor
IT PBS
IT DT
IT PBS
IT DT
44.7
7.2
CD25
FoxP3
C
MC38
IT PBS (0/5 CR)
IT DT (4/5 CR)
mm3
1500
1000
500
***
-10 0 10 20 30
Days after IT DT
IT PBS
IT DT
D
B16F10
IT PBS (0/7 CR)
IT DT (4/5 CR)
2000
1500
1000
500
E
Sarcoma Treg Frequency
%FoxP3+CD25+ of CD4+
50
40
30
20
10
0
**
Foxp3WT
Foxp3DTR
+ IT DT
F
Survival: KP Sarcoma
Foxp3WT + IT DT
Foxp3DTR + IT DT
*
Overall Survival
100
75
50
25
0
4/14 CR
0/9 CR
0
50
100
150
Days after IT DT

Figure 1. Intratumoral Treg depletion is sufficient to control tumor growth.
(A) Experimental design for intratumoral diphtheria toxin (IT DT) injection in *Foxp3*^{DTR} mice. DT was administered every 48-72 hours beginning when tumors were 50mm^3 and throughout the study.
(B) IT Treg frequencies in MC38 tumor-bearing *Foxp3*^{DTR} mice 48 hours after one dose of IT PBS or IT DT. Representative flow cytometric staining for FoxP3+ CD25+ Tregs of live CD4+ T cells.
(C-D) MC38 tumor growth (C) or B16F10 tumor growth (D) in *Foxp3*^{DTR} mice after sustained IT DT or IT PBS treatment. Data are representative of 4-10 independent experiments for each tumor type.
(E) IT Treg frequencies in IT DT treated *K-ras*^{G12D}*;p53*$^{-/-}$ versus *Foxp3*$^{DTR-GFP}$*;K-ras*^{G12D}*;p53*$^{-/-}$ autochthonous sarcomas.
(F) Survival analysis of sarcoma-bearing mice after IT DT treatment beginning when palpable mass was detected.
Data represent means ± SEM; *$p < 0.05$, **$p < 0.01$ and ***$p < 0.001$. B,F: Unpaired two-tailed T test. C,D: Ordinary two-way ANOVA with Tukey's multiple comparison test. G: One-sided Chi-square test. (n=5-14 mice/group).

FIGURE 2

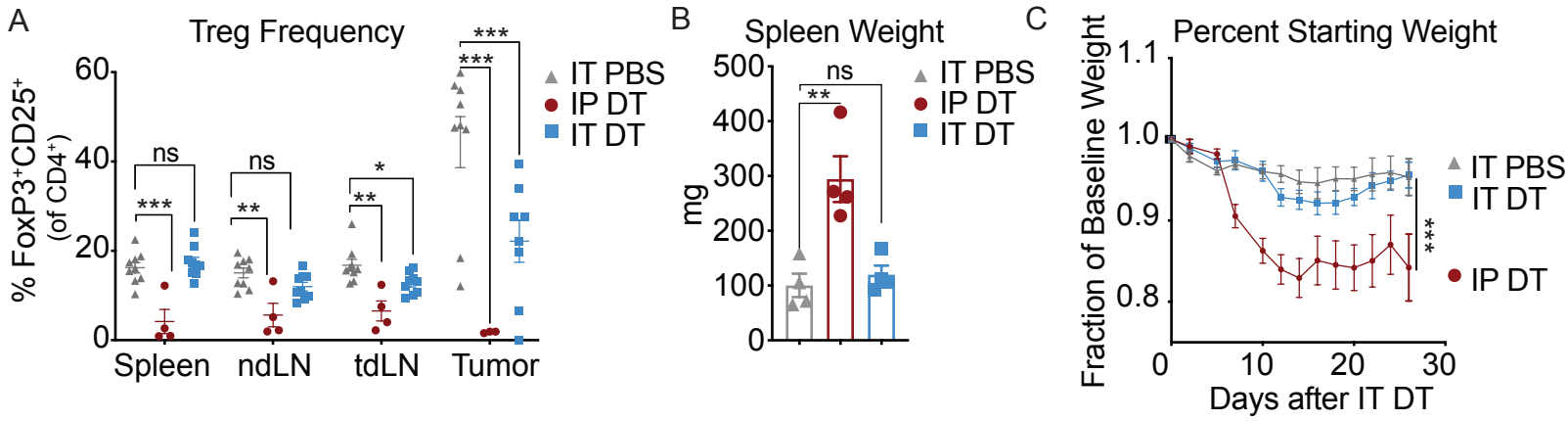

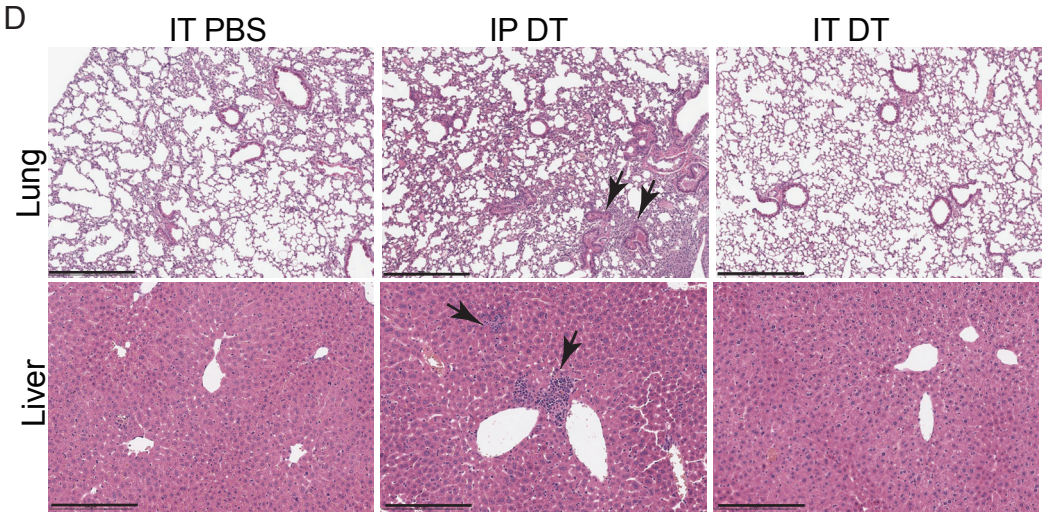

E

Pathology score: severely damaged (++), damaged (+), normal (-)

Group	Sample ID	Lung	Liver	Treatment
1	494	+	-	IT PBS
	495	+	-	
2	238	+	+	IP DT
	386	++	+	
3	239	-	-	IT DT
	385	-	-	

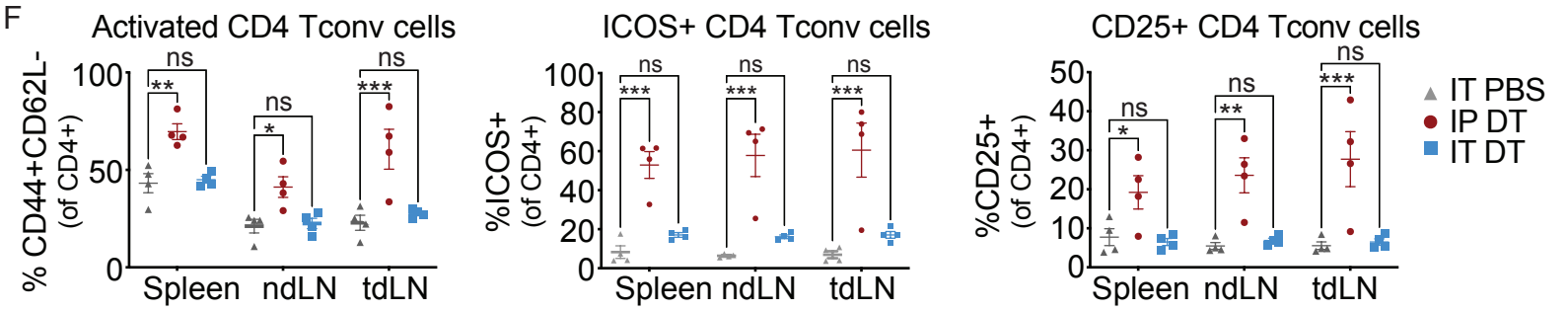

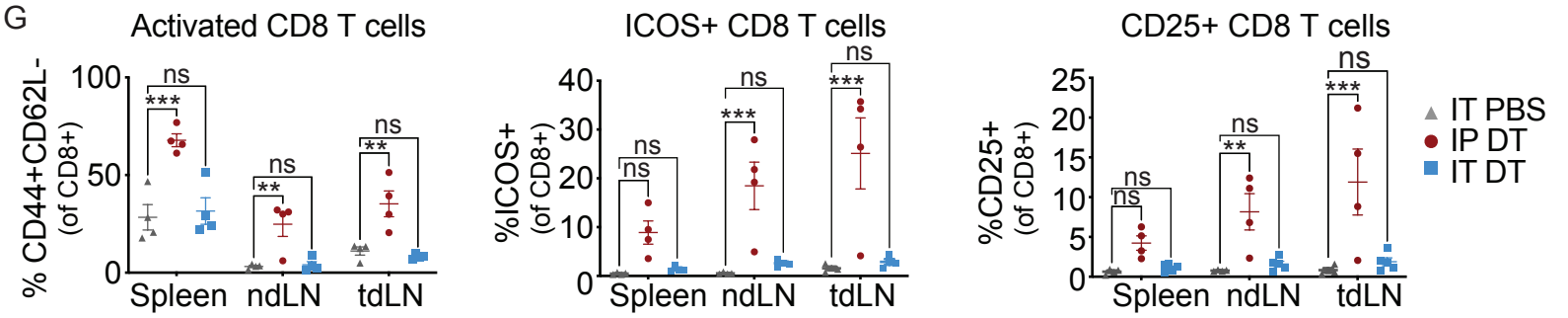

Figure 2. IT Treg ablation, unlike systemic Treg ablation, does not cause autoimmune pathology.

(A) Treg frequencies in spleen, non-tumor-draining lymph nodes (ndLN), tumor-draining LN (tdLN), and tumor after IP PBS, IP DT, or IT DT in MC38-tumor bearing *Foxp3*^{DTR} mice.

(B) Spleen weight in MC38-tumor bearing *Foxp3*^{DTR} mice after 30 days of sustained IP or IT DT treatment.

(C) Body weight of MC38-tumor bearing *Foxp3*^{DTR} mice treated with IP PBS, IP DT, or IT DT.

(D) Hematoxylin and eosin staining performed on lung and liver tissues harvested after sustained IP PBS, IP DT, or IT DT. Arrows indicate lymphocytic infiltrates within tissues. Images are representative of two biological replicates for each treatment group.

(E) Pathology scores of IT PBS, IP DT or IT DT treated mice.

(F-G) Percent of CD4+ (F) and CD8+ (G) T cells expressing CD44, ICOS, and CD25 activation markers after sustained IP PBS, IP DT, or IT DT.

Data are representative of 3 independent experiments. Data represent means ± SEM; *$p < 0.05$, **$p < 0.01$ and ***$p < 0.001$. A,B: Unpaired two-tailed T test. C;F;G: Ordinary two-way ANOVA with Tukey's multiple comparison test. (n=4-9 mice/group).

FIGURE 3

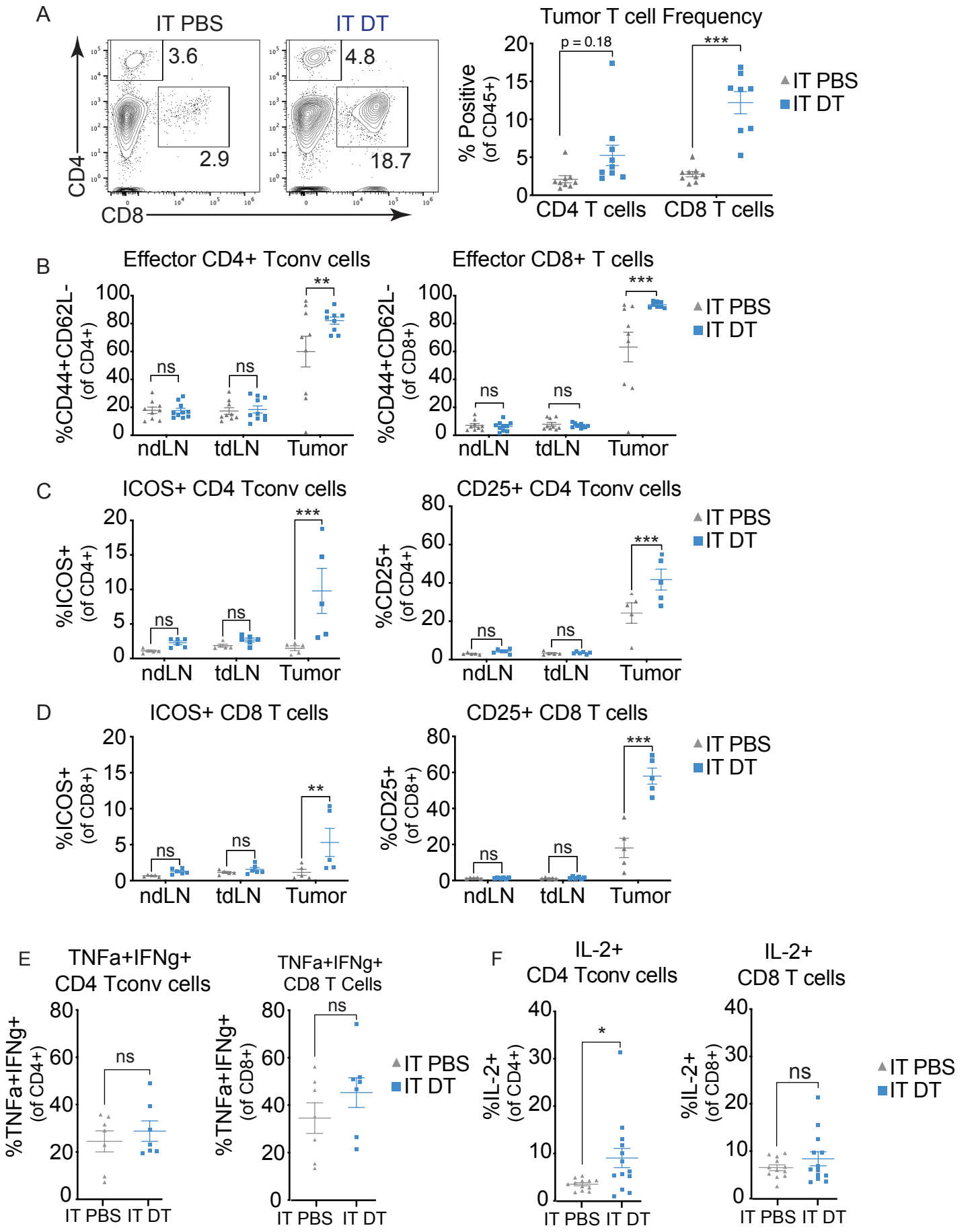
A
IT PBS
IT DT
3.6
2.9
4.8
18.7
CD4
CD8
Tumor T cell Frequency
% Positive (of CD45+)
p = 0.18
***
CD4 T cells
CD8 T cells
IT PBS
IT DT
B
Effector CD4+ Tconv cells
%CD44+CD62L- (of CD4+)
ns
ns
**
ndLN
tdLN
Tumor
Effector CD8+ T cells
%CD44+CD62L- (of CD8+)
ns
ns
***
C
ICOS+ CD4 Tconv cells
%ICOS+ (of CD4+)
***
CD25+ CD4 Tconv cells
%CD25+ (of CD4+)
***
D
ICOS+ CD8 T cells
%ICOS+ (of CD8+)
**
CD25+ CD8 T cells
%CD25+ (of CD8+)
***
E
TNFa+IFNg+ CD4 Tconv cells
%TNFa+IFNg+ (of CD4+)
ns
TNFa+IFNg+ CD8 T Cells
%TNFa+IFNg+ (of CD8+)
ns
IT PBS
IT DT
F
IL-2+ CD4 Tconv cells
%IL-2+ (of CD4+)
*
IL-2+ CD8 T cells
%IL-2+ (of CD8+)
ns

Figure 3. IT Treg depletion promotes CD8 and CD4 T cell activation locally in tumors.
(A) Representative flow plots and quantification of CD4+ Tconv and CD8+ T cell frequencies in tumor tissue after sustained PBS or IT DT treatment.
(B) Frequencies of effector (CD44+CD62L-) CD4+ Tconv cell or CD8+ T cells after IT PBS or IT DT.
(C-D)Percentages of CD44+, ICOS+ or CD25+ on CD4+ Tconv cells or (D) CD8+ T cells.
(E) TNFα and IFNγ cytokine expression in tumor-infiltrating CD8+ and CD4+ Tconv cells.
(F) IL-2 cytokine expression in CD4+ Tconv or CD8 T cells after PBS or IT DT treatment.
Data are representative of 2 independent experiments. Data represent means ± SEM; *$p < 0.05$, **$p < 0.01$ and ***$p < 0.001$. A: Unpaired two-tailed T test. B-F: Ordinary two-way ANOVA with Tukey's multiple comparison test. (n=5-10 mice/group).

FIGURE 4

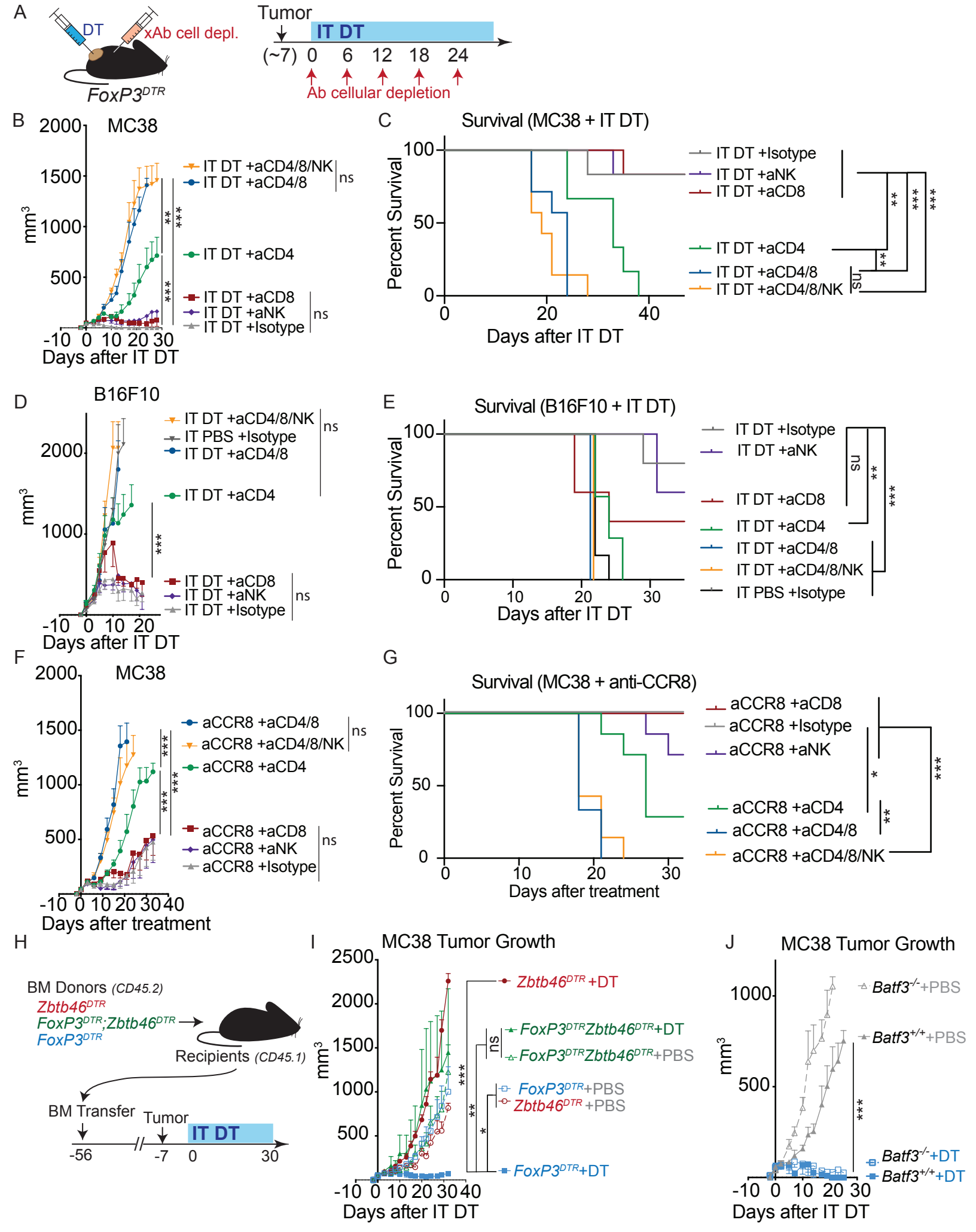
A
DT
xAb cell depl.
FoxP3DTR
Tumor
IT DT
(~7) 0 6 12 18 24
Ab cellular depletion
B
MC38
mm3
IT DT +aCD4/8/NK
IT DT +aCD4/8
ns
IT DT +aCD4
IT DT +aCD8
IT DT +aNK
IT DT +Isotype
ns
Days after IT DT
C
Survival (MC38 + IT DT)
Percent Survival
IT DT +Isotype
IT DT +aNK
IT DT +aCD8
IT DT +aCD4
IT DT +aCD4/8
IT DT +aCD4/8/NK
Days after IT DT
D
B16F10
mm3
IT DT +aCD4/8/NK
IT PBS +Isotype
IT DT +aCD4/8
ns
IT DT +aCD4
IT DT +aCD8
IT DT +aNK
IT DT +Isotype
ns
Days after IT DT
E
Survival (B16F10 + IT DT)
Percent Survival
IT DT +Isotype
IT DT +aNK
IT DT +aCD8
IT DT +aCD4
IT DT +aCD4/8
IT DT +aCD4/8/NK
IT PBS +Isotype
Days after IT DT
F
MC38
mm3
aCCR8 +aCD4/8
aCCR8 +aCD4/8/NK
ns
aCCR8 +aCD4
aCCR8 +aCD8
aCCR8 +aNK
aCCR8 +Isotype
ns
Days after treatment
G
Survival (MC38 + anti-CCR8)
Percent Survival
aCCR8 +aCD8
aCCR8 +Isotype
aCCR8 +aNK
aCCR8 +aCD4
aCCR8 +aCD4/8
aCCR8 +aCD4/8/NK
Days after treatment
H
BM Donors (CD45.2)
Zbtb46DTR
FoxP3DTR;Zbtb46DTR
FoxP3DTR
Recipients (CD45.1)
BM Transfer
Tumor
IT DT
-56 -7 0 30
I
MC38 Tumor Growth
mm3
Zbtb46DTR +DT
FoxP3DTRZbtb46DTR+DT
FoxP3DTRZbtb46DTR+PBS
ns
FoxP3DTR+PBS
Zbtb46DTR +PBS
FoxP3DTR+DT
Days after IT DT
J
MC38 Tumor Growth
mm3
Batf3-/-+PBS
Batf3+/+PBS
Batf3-/-+DT
Batf3+/+DT
Days after IT DT

Figure 4. Conventional CD4+ T cells control tumors after IT Treg ablation.
(A) Experimental design for cellular depletion studies in *Foxp3*^{DTR} mice. IT Treg ablation was achieved through either IT DT or anti-CCR8 and began concurrent with cellular depletion. *In vivo* depletion antibodies were administered IP every 6 days for the duration of the study.
(B) MC38 tumor growth in *Foxp3*^{DTR} mice that received IT DT and indicated cellular depleting antibodies.
(C)Animal survival after IT DT treatment and indicated cellular depletion. One experiment performed.
(D) B16F10 tumor growth in *Foxp3*^{DTR} mice that received IT DT and indicated cellular depleting antibodies.
(E) Animal survival after IT DT and indicated cellular depletion. One experiment performed.
(F) MC38 tumor growth after anti-CCR8 treatment and indicated cellular depletion.
(G) Animal survival after anti-CCR8 and cellular depletion. One experiment performed.
(H) Schematic of bone marrow chimera generation and treatment regimen in *Zbtb46*^{DTR}*Foxp3*^{DTR} chimeric mice. 250 ng IT DT and 80 ng IP DT was administered every 48-72 hours, once MC38 tumors reached 50mm^3.
(I) MC38 tumor growth in *Zbtb46*^{DTR}*Foxp3*^{DTR} chimeric mice. One experiment performed.
(J) MC38 tumor growth in *Foxp3*^{DTR}*Batf3*$^{-/-}$ mice. 250 ng IT DT was administered every 48-72 hours. Data are representative of 3 independent experiments.
Data represent means ± SEM; *$p < 0.05$, **$p < 0.01$ and ***$p < 0.001$. B,D,F; I-J: Ordinary two-way ANOVA with Tukey's multiple comparison test. C,E,J: Log-rank (Mantel-Cox) test. (n=5-7 mice/group).

FIGURE 5

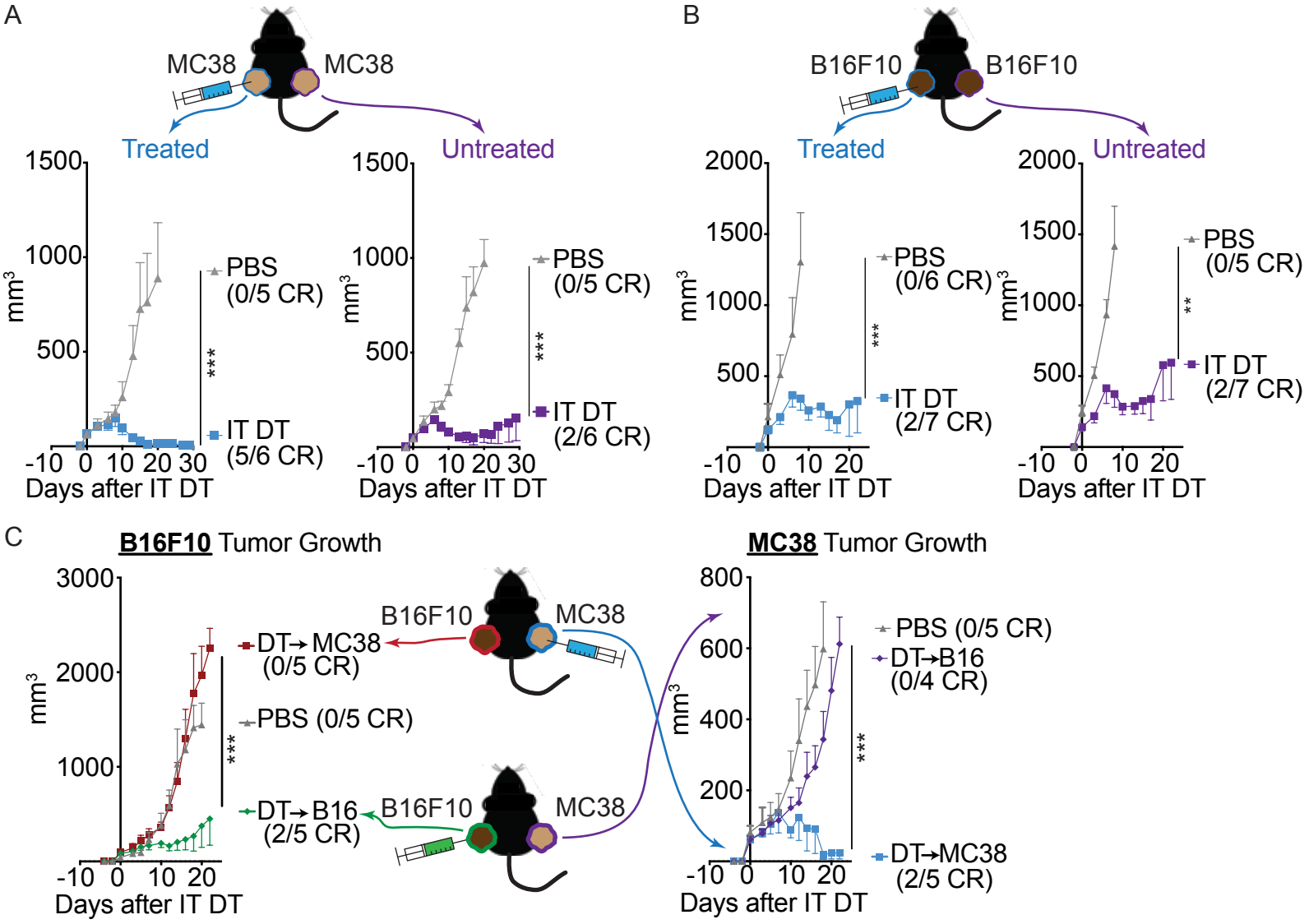
A
MC38
MC38
Treated
Untreated
1500
1000
500
mm3
PBS (0/5 CR)
IT DT (5/6 CR)
***
-10 0 10 20 30
Days after IT DT
PBS (0/5 CR)
IT DT (2/6 CR)
B
B16F10
B16F10
2000
1500
1000
500
PBS (0/6 CR)
IT DT (2/7 CR)
PBS (0/5 CR)
IT DT (2/7 CR)
**
-10 0 10 20
C
B16F10 Tumor Growth
MC38 Tumor Growth
3000
2000
1000
DT→MC38 (0/5 CR)
PBS (0/5 CR)
DT→B16 (2/5 CR)
B16F10
MC38
800
600
400
200
PBS (0/5 CR)
DT→B16 (0/4 CR)
DT→MC38 (2/5 CR)

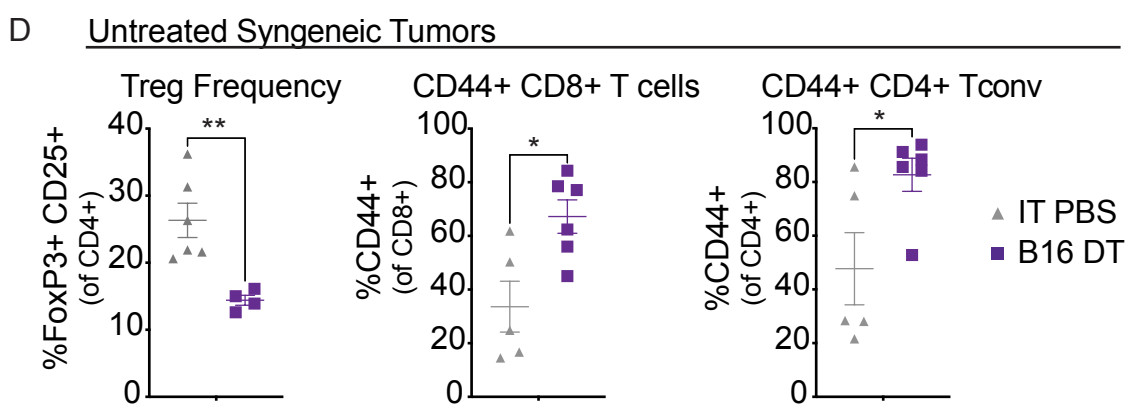
D
Untreated Syngeneic Tumors
Treg Frequency
CD44+ CD8+ T cells
CD44+ CD4+ Tconv
%FoxP3+ CD25+ (of CD4+)
%CD44+ (of CD8+)
%CD44+ (of CD4+)
40
30
20
10
0
100
80
60
40
20
0
**
*
IT PBS
B16 DT

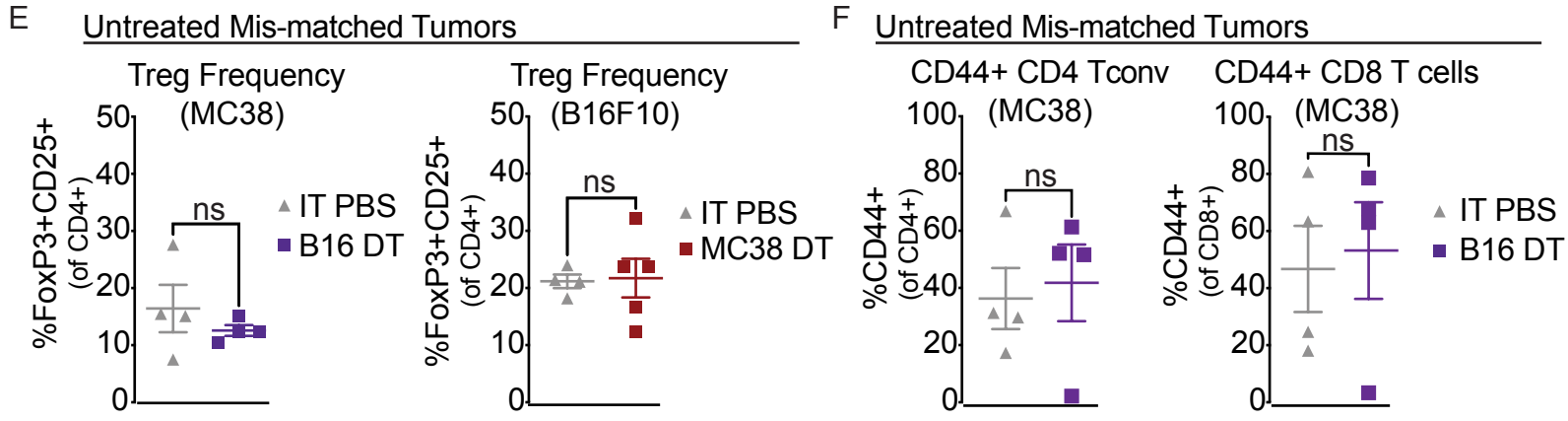
E
Untreated Mis-matched Tumors
Treg Frequency (MC38)
Treg Frequency (B16F10)
%FoxP3+CD25+ (of CD4+)
50
40
30
20
10
0
ns
IT PBS
B16 DT
MC38 DT
F
Untreated Mis-matched Tumors
CD44+ CD4 Tconv (MC38)
CD44+ CD8 T cells (MC38)
%CD44+ (of CD4+)
%CD44+ (of CD8+)
100
80
60
40
20
0

Figure 5. Ablation of IT Tregs in a single tumor unleashes antitumor immunity against syngeneic distal tumors.

(A) MC38 tumor growth of an IT DT treated tumor and a distal, MC38 untreated tumor.
(B) B16F10 tumor growth of an IT DT treated tumor and a distal, untreated B16F10 tumor.
(C) B16F10 or MC38 tumor growth in *Foxp3*^{DTR} mice bearing an MC38 tumor on the right flank and a B16F10 tumor on the left flank. B16F10 tumors are directly treated (green) or MC38 tumors are directly treated (blue). Data are representative of 5 independent experiments.
(D) Quantification of Treg and activated CD4+ Tconv cell and CD8+ T cell frequencies in matched B16F10-tumor bearing mice.
(E-F) Quantification of Treg frequencies or (F) activated CD4+ Tconv cells and CD8+ T cells in untreated MC38 or B16F10 tumors after IT DT in a mismatched B16F10 or MC38 tumor, respectively.
Data are representative of 5 independent experiments for matched MC38 tumors and 2 independent experiments for matched B16F10 tumors. Data represent means ± SEM; *$p < 0.05$, **$p < 0.01$ and ***$p < 0.001$. A-C: Ordinary two-way ANOVA with Tukey's multiple comparison test. D-F: Unpaired two-tailed T test. (n=4-7 mice/group).

FIGURE 6

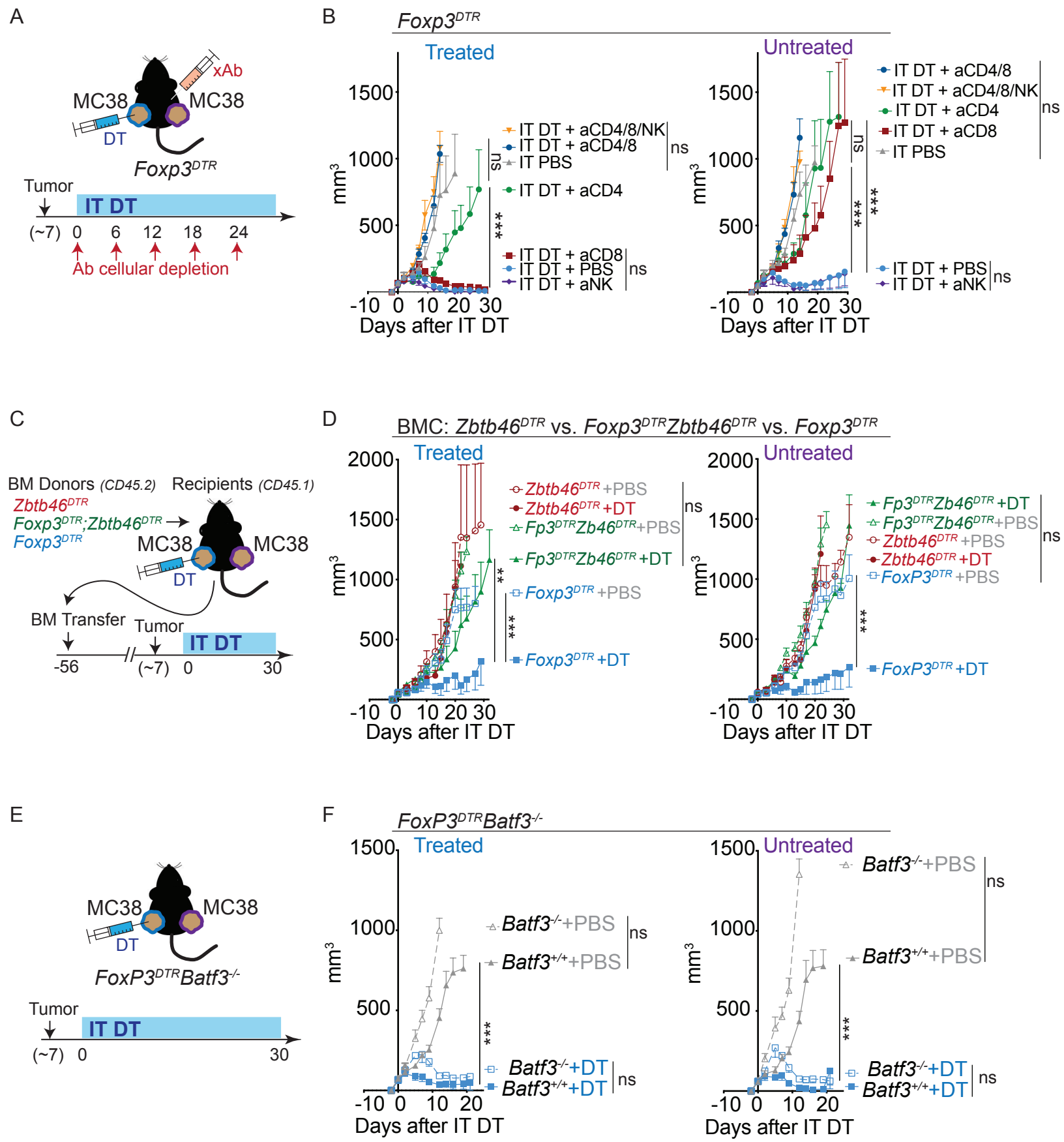
A
xAb
MC38
MC38
DT
Foxp3DTR
Tumor
IT DT
(~7) 0 6 12 18 24
Ab cellular depletion
B
Foxp3DTR
Treated
Untreated
mm3
Days after IT DT
IT DT + aCD4/8/NK
IT DT + aCD4/8
IT PBS
IT DT + aCD4
IT DT + aCD8
IT DT + PBS
IT DT + aNK
ns
***
C
BM Donors (CD45.2)
Recipients (CD45.1)
Zbtb46DTR
Foxp3DTR;Zbtb46DTR
Foxp3DTR
MC38
MC38
DT
BM Transfer
Tumor
IT DT
-56
(~7) 0 30
D
BMC: Zbtb46DTR vs. Foxp3DTRZbtb46DTR vs. Foxp3DTR
Treated
Untreated
Zbtb46DTR +PBS
Zbtb46DTR +DT
Fp3DTRZb46DTR+PBS
Fp3DTRZb46DTR +DT
Foxp3DTR +PBS
Foxp3DTR +DT
FoxP3DTR +PBS
FoxP3DTR +DT
**
E
MC38
MC38
DT
FoxP3DTRBatf3-/-
Tumor
IT DT
(~7) 0 30
F
FoxP3DTRBatf3-/-
Treated
Untreated
Batf3-/-+PBS
Batf3+/+PBS
Batf3-/-+DT
Batf3+/+DT

Figure 6. Control of disseminated tumors is reversed by CD8+ or CD4+ T cell depletions.
(A) Schematic of tumor inoculation and cellular depletion regimen in *Foxp3*^{DTR} mice.
(B) MC38 tumor growth of an IT DT treated tumor or distal, untreated tumor.
(C) Experimental schematic of *Zbtb46*^{DTR}*Foxp3*^{DTR} bone marrow chimera generation.
(D) MC38 tumor growth in *Zbtb46*^{DTR}*Foxp3*^{DTR} bone marrow chimeric mice. One experiment performed.
(E) Experimental setup of IT Treg depletion in *Foxp3*^{DTR}*Batf3*$^{-/-}$ mice.
(F) MC38 tumor growth in an IT DT treated tumor or a distal, untreated tumor in *Foxp3*^{DTR}*Batf3*$^{-/-}$ mice. One experiment performed.
Data are representative of 2-5 independent experiments. Data represent means ± SEM; *$p < 0.05$, **$p < 0.01$ and ***$p < 0.001$. B-G: Ordinary two-way ANOVA with Tukey's multiple comparison test. (n=4-7 mice/group).

FIGURE 7

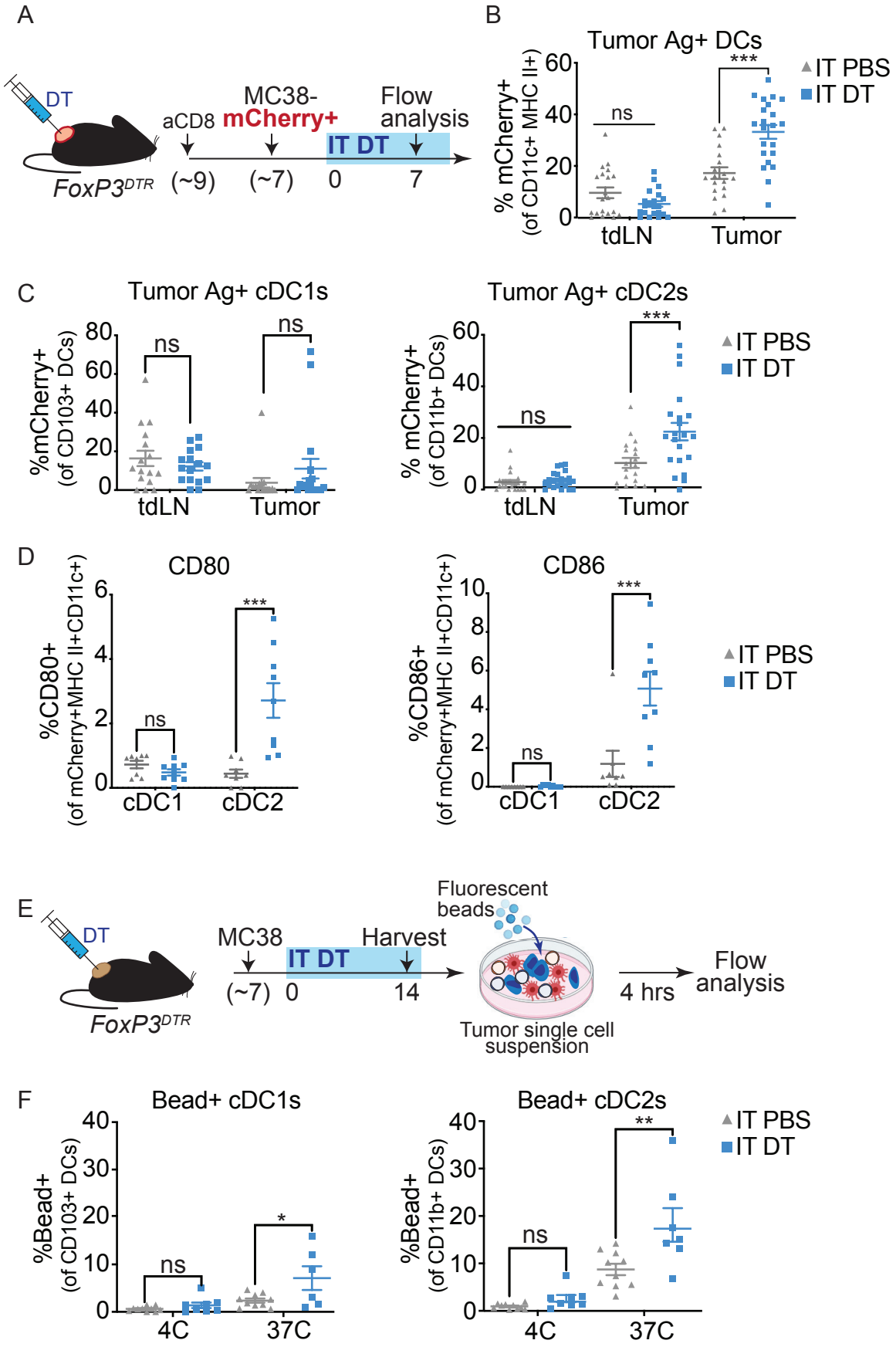
A
DT
FoxP3DTR
aCD8
MC38-
mCherry+
Flow
analysis
IT DT
(~9)
(~7)
0
7
B
Tumor Ag+ DCs
% mCherry+
(of CD11c+ MHC II+)
ns
***
tdLN
Tumor
IT PBS
IT DT
C
Tumor Ag+ cDC1s
%mCherry+
(of CD103+ DCs)
Tumor Ag+ cDC2s
% mCherry+
(of CD11b+ DCs)
D
CD80
%CD80+
(of mCherry+MHC II+CD11c+)
CD86
%CD86+
(of mCherry+MHC II+CD11c+)
cDC1
cDC2
E
MC38
Harvest
Fluorescent
beads
Tumor single cell
suspension
4 hrs
Flow
analysis
F
Bead+ cDC1s
%Bead+
(of CD103+ DCs)
Bead+ cDC2s
%Bead+
(of CD11b+ DCs)
4C
37C
*
**

Figure 7. IT Treg ablation enhances tumor antigen acquisition by cDC2s.
(A)Experimental schematic. *Foxp3*^{DTR} mice received anti-CD8 depleting antibodies two days prior to mCherry+ MC38 tumor inoculation and every six days thereafter. IT DT began when tumors reached 50mm^3.
(B) Quantification of mCherry+ DCs after IT PBS or IT DT treatment.
(C) Quantification of mCherry+ cDC1s or cDC2s in tumor and tdLNs.
(D) Quantification of CD80 and CD86 expression on mCherry+ cDC1s and mCherry+ cDC2s.
(E) Schematic of experimental approach in *ex vivo* assays. *Foxp3*^{DTR} mice were inoculated with MC38 tumors and dosed with IT DT when tumors reached 50mm^3. Tumors were harvested and plated with fluorescent beads after seven days of IT DT treatments.
(F) Frequencies of cDC1s or cDC2s that phagocytosed beads at either 4C or 37C.
In vivo data are representative of 2 independent experiments. *Ex vivo* data are representative of 3 independent experiments. Data represent means ± SEM; *$p < 0.05$, **$p < 0.01$ and ***$p < 0.001$. B-E; G,H: Ordinary two-way ANOVA with Tukey's multiple comparison test. (n=4-7 mice/group).